SYNTHESIS AND SWELLING-RELEASE BEHAVIOR OF SUPERABSORBENT NANOCOMPOSITES
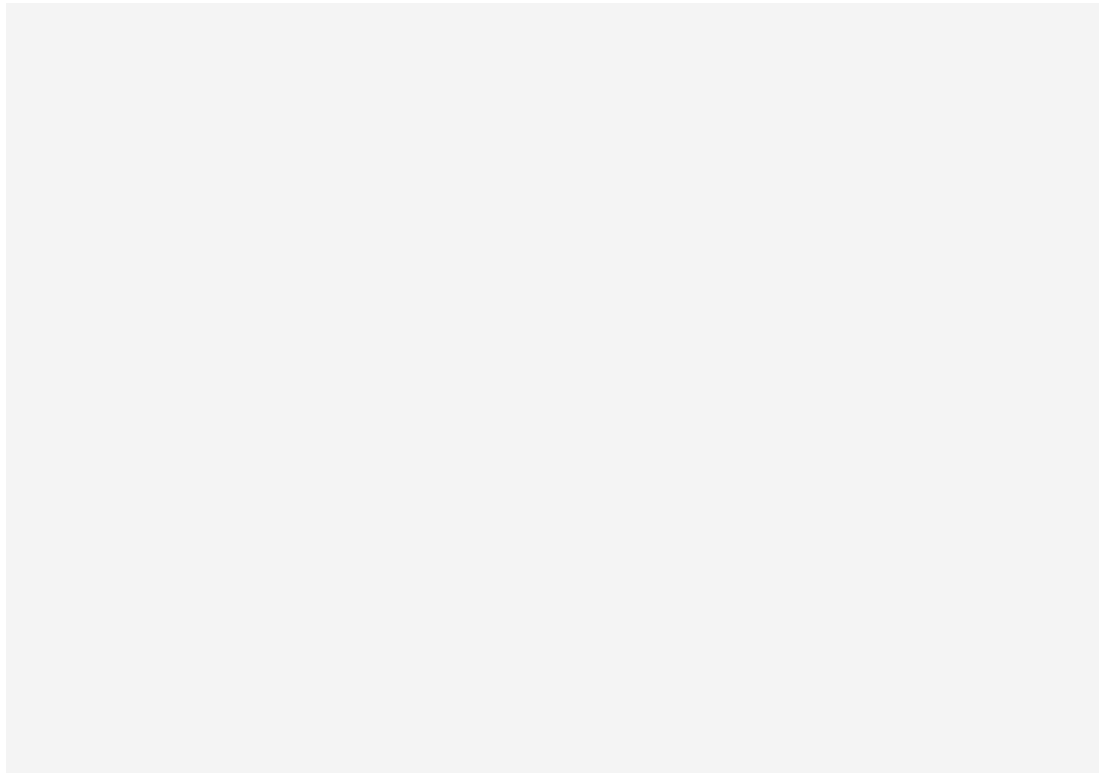
by

YEŞİM MENCELOĞLU

Submitted to the Graduate School of Engineering and Natural Sciences
in partial fulfillment of the requirements for the degree of
Master of Science

SABANCI UNIVERSITY

December 2021

SYNTHESIS AND SWELLING-RELEASE BEHAVIOR OF SUPERABSORBENT NANOCOMPOSITES

Approved by:

Date of Approval: December 16, 2021

YEŞİM MENCELOĞLU 2021 ©

To my family

ABSTRACT
SYNTHESIS AND SWELLING-RELEASE BEHAVIOR OF SUPERABSORBENT NANOCOMPOSITES

Yeşim Menceloğlu

Materials Science and Nanoengineering, MSc. Thesis, 2021

Thesis Supervisor: Prof. Dr. Yusuf Ziya Menceloğlu

Keywords: Superabsorbent polymers, equilibrium swelling ratios, crosslink density, storage modulus, Halloysite Nanotubes

Superabsorbent polymers (SAPs) are functional polymers in various application fields from the hygiene industry to construction and agriculture. As versatility and high water absorption capacity are significant merits, SAPs usually suffer from low water retention capacity (fast release) and weak mechanical properties. To address these drawbacks, a set of new superabsorbent polymer – Halloysite nanotubes (HNT) nanocomposites were synthesized via free radical polymerization of acrylamide, 2-acrylamido-2-methylpropane-1-sulfonic acid and acrylic acid in the presence of vinyltrimethoxysilane (VTMS) as the crosslinker. FTIR and TGA characterizations confirm the polymerization of SAP and the successful incorporation of HNT into the SAP polymer matrix. The effect of different amounts of HNT nanofiller addition into nanocomposite polymer matrix was investigated with swelling-release performance tests, crosslink density calculations, and rheology measurement. It is found out that equilibrium swelling ratios are correlated, and therefore can be tuned via crosslinking densities of nanocomposites, while water retention capacities are governed by storage moduli. A maximum swelling of 537 g/g was observed 5% HNT was incorporated, in which the crosslinking density is the lowest. Among the SAP nanocomposites prepared, the highest storage modulus was observed when 1% of nanofiller was included, which coincides with the

longest water retention nanocomposite. The water release duration of SAPs was prolonged up to 27 days with 1% HNT addition in parallel with the approached maximum storage modulus. Finally, three different incorporation mechanisms of HNT nanofiller into SAP nanocomposite structure were proposed and confirmed with rheology measurements. Moreover, another SAP data set were synthesized with other Poly(ethylene glycol) diacrylate crosslinking agents to observe the effect of crosslinker chain length and amount on crosslinking density and the correlation between crosslinking density and equilibrium swelling capacity. This study provides a rapid synthesis method for SAP nanocomposites with enhanced water retention capacities and explains the relationship between swelling-crosslink density and water retention-mechanical properties of SAP nanocomposites. In addition, the second SAP set with tunable crosslinking densities was prepared with PEGDA crosslinkers and was explained the swelling-crosslink density correlation in detail.

ÖZET

SÜPER ABSORBAN NANOKOMPOZİT HİDROJELLERİN SENTEZİ VE ŞİŞME-SALINIM PERFORMANLARININ İNCELENMESİ

Yeşim Menceloğlu

Malzeme Bilimi ve Nanomühendisliği, Yüksek Lisans Thesis, 2021

Tez danışmanı: Prof. Dr. Yusuf Ziya Menceloğlu

Anahtar Kelimeler: Süper emici polimerler, denge şişme oranları, çapraz bağ yoğunluğu, depolama modülü, Halloysit Nanotüpler

Süper emici polimerler (SAP'ler), hijyen endüstrisinden inşaat ve tarıma kadar çeşitli uygulama alanlarında fonksiyonel polimerlerdir. SAP'ler genellikle düşük su tutma kapasitesi (hızlı salınım) ve zayıf mekanik özelliklerden muzdarip olduğundan, çok fonksiyonluluk ve yüksek su emme kapasitesi önemli avantajlarındandır. Bu dezavantajları gidermek için, viniltrimetoksisilan(VTMS) çapraz bağlayıcısı varlığında akrilamid, 2-akrilamido-2-metilpropan-1-sülfonik asit ve akrilik asidin serbest radikal polimerizasyonu yoluyla bir dizi yeni süper emici polimer – Halloysit nanotüpler (HNT) nanokompozitleri sentezlendi. FTIR ve TGA karakterizasyonları, SAP'nin polimerizasyonunu ve HNT'nin SAP polimer matrisine başarılı bir şekilde dahil edilmesini onaylar. Nanokompozit polimer matrisine farklı miktarlarda HNT nanodolgu ilavesinin etkisi şişme-serbest bırakma performans testleri, çapraz bağ yoğunluğu hesaplamaları ve reoloji ölçümü ile araştırılmıştır. Dengedeki şişme oranlarının çapraz bağlanma yoğunluğuyla ilişkili olduğu ve nanokompozitlerin çapraz bağlanma yoğunlukları ile maksimum şişme kapasitelerinin ayarlanabileceği, su tutma kapasitelerinin ise depolama modülleri tarafından yönetildiği bulunmuştur. Çapraz bağlama yoğunluğu en düşük olan % 5 HNT dahil edildiğinde , 537 g/g'lik bir maksimum şişme gözlemlenmiştir. Hazırlanan SAP nanokompozitleri arasında en yüksek depolama modülü, en uzun su tutma nanokompozitine denk gelen %1 nanofiller dahil edildiğinde gözlenmiştir. Yaklaşan maksimum depolama modülüne paralel olarak SAP'lerin su bırakma süresi %1 HNT ilavesiyle 27 güne kadar uzatılmıştır. Son olarak, HNT nanodolgu maddesinin SAP

nanokompozit yapısına üç farklı dahil etme mekanizması önerilmiş ve reoloji ölçümleri ile doğrulanmıştır. Çapraz bağlayıcı zincir uzunluğu ve miktarının çapraz bağlama yoğunluğu üzerindeki etkisini ve çapraz bağlama yoğunluğu ile denge şişme kapasitesi arasındaki korelasyonu gözlemlemek için diğer SAP veri seti Poli(etilen glikol) diakrilat çapraz bağlayıcılarıyla sentezlenmiştir. Bu çalışma, gelişmiş su tutma kapasitelerine sahip SAP nanokompozitleri için hızlı bir sentez yöntemi sağlar ve SAP nanokompozitlerinin şişme-çapraz bağ yoğunluğu ile su tutma-mekanik özellikleri arasındaki ilişkiyi açıklamaktadır. Ayrıca PEGDA çapraz bağlayıcıları ile ayarlanabilir çapraz bağlanma yoğunluklarına sahip ikinci SAP seti hazırlanmış ve şişme-çapraz bağ yoğunluğu korelasyonu detaylı olarak anlatılmıştır.

ACKNOWLEDGEMENTS

First of all, I would like to express my sincere gratitude to my supervisor Prof. Dr. Yusuf Ziya Menceloğlu, for his invaluable advice, dedicated support, and guidance during my Master's study.

I would like to thank Dr. Merve Senem Seven for her consistent support and recommendations on this dissertation.

I am deeply grateful to Ekin Berksun for her friendly support, motivation, and endless help in all matters. It was a great pleasure to work with Deniz Anıl during our funny times with 2-roll in 2107.

Thanks should also go to Damla Aksoy Kızılkoca for our unforgettable study times with long coffee breaks.

Special thanks to my research team members, Ogeday Rodop, Çağla Girişken, Bilgen Aktaş, Ceyda Yanmaz, Gizem Arıtürk, Gülşah Yıldız and Gizem Kurtulmuş for our enjoyable time spent together in pizza party meetings.

I would like to thank to my collegues, Ayşe Durmuş Sayar, Yelda Yorulmaz, Erdinç Taş, Buket Taş, Billur Seviniş, Onur Zırhlı, Doğacan Kızılkoca, Tuğçe Akkaş, Aysu Yurduşen, İpek Bilge and Kadriye Kahraman for their friendship and support.

Finally and most importantly, a heartfelt thank goes to my family and my fiance for their unwavering support and belief in me. A special thank you to my fiance, who continues to support and motivate me despite all my complaints and whinings. It would be impossible to complete my study without their endless support.

TABLE OF CONTENTS

LIST OF FIGURES

LIST OF TABLES

LIST OF EQUATIONS

LIST OF ABBREVIATIONS

HNT: Halloysite Nanotube

AM: Acrylamide

AMPS: 2-Acrylamido-2-methylpropane-1-sulfonic acid

AA: Acrylic Acid

VTMS: Vinyltrimethoxysilane

APS: Ammonium persulfate

FTIR: Reflectance Fourier Transformed Infrared Spectroscopy

TGA: Thermo Gravimetric Analysis

DSC: Differential Scanning Calorimetry

GPC: Gel Permeation Chromatography

NMR: Nuclear Magnetic Resonance Spectroscopy

XL: Crosslink

Mc: Molecular weight between crosslinks

H_m: Melting Enthalpy

H_c: Crystallization Enthalpy

W_s: Swollen weight of SAP

W_d: Dry weight of SAP

Chapter 1

1. Introduction

Super-absorbent polymers (SAP) are lightly crosslinked hydrophilic polymers with thousands of times their weight aqueous adsorption capacity thanks to their three-dimensional crosslinked polymer structure [1]. The investigation of super-absorbent polymer preparation had based on the 1930s when W. Kern performed the thermal polymerization of the poly(acrylic acid) crosslinked with divinylbenzene [2]. First, the enhancement of SAP was done in the Northern Regional Laboratory of the US Department of Agriculture in the 1970s. Then, in 1972 patent, Harper and coworkers claimed the use of crosslinked acrylate-based crosslinked polymers as absorbents in diapers, personal care products. The SAP production capacities had gradually increased, and at the end of the 1990s reached approximately one million tons globally [2, 3].

In the beginning, the utilization of SAPs as a water reservoir made them attractive in agriculture for promoting plant protection under water scarcity. Still, as the personal care product industry had a more marketplace, the use of SAPs in diapers became more favorable in a short time. Although 80 % of the super-absorbent polymers are produced for personal care products like diapers, sanitary pads, during the last years, they have been being used in various application areas such as notably agriculture [4], tissue engineering [5], food packing [6], drug delivery [7], adhesives [8], wastewater treatment [9]. The reasons behind the uniqueness and smartness of hydrogels are their characteristic response to external stimuli such as pH [10], ionic strength [11], solvent composition, temperature, and light [12, 13]. The high-water absorption capacity, biocompatibility, softness, and sensitiveness to environmental stimuli make SAPs preferable for a wide variety of applications.

The water absorption and retention properties of SAPs are results of 3-dimensional crosslinked polymer structure and the hydrophilic functional end groups on the polymer chains. They swell right after contact with water due to the differences in osmotic pressure and the presence of hydrophilic functional groups such as -OH, -COOH, -CONH-, -CHO, -COONa, -SO3H, -NH2 in the polymer backbone. The reason behind SAPs swelling instead of dissolution in aqueous medium is the chemical or physical crosslinking introduced into polymer network structure via a crosslinker during or after the polymerization. This way,

crosslinked SAPs are able to absorb large amount of water and hold in their 3D structure [5, 12, 14].

The preparations of SAPs are based on two different sources decided according to desired properties and/or application areas. SAPs are classified as natural or synthetic with respect to their sources. Cellulose [14], starch [15], collagen [16], alginate [17], and chitosan [18] are some examples of SAPs from natural sources [13]. On the other hand, acrylamide [19, 20], acrylic acid [19, 21], methacrylic acid [22], hydroxyethyl-methacrylate [23], polyvinyl alcohol [24], and various acrylates are commonly used in the synthesis of synthetic SAPs. The maximum swelling capacities, Their higher absorption capacities [25], more durable gel life [26] and higher mechanical strength [27] properties make synthetic super-absorbent polymers more preferable than natural ones. In some cases, combined SAPs can be prepared using both natural and synthetic polymers. [28] These are generally synthesized via graft polymerization [29].

1.1. The Main Aim and Objectives

Super-absorbent polymers (SAPs) are functional polymers in a wide range of application fields from the hygiene industry to construction and agriculture. However, as versatility and high water absorption capacity are their important merits, SAPs usually suffer from low water retention capacity (fast release) and weak mechanical properties. Low elastic modulus, low fracture energies, negligible fatigue resistance are the main problems of super-absorbent polymers, which effects the swelling / release ratios and aqueous retention performance under load [30]. The weak and brittle mechanical properties of SAPs are the results of not to be dissipated energy effectively in the 3D polymer network [31]. In addition to that, molecular weight between crosslinks is not uniform since the crosslinking points are placed disorderly in the polymer network. Therefore, the stress cannot be dissipated in the intrinsic structure and microcracks form [32]. To address these drawbacks, a set of new super-absorbent polymer – Halloysite nanotubes (HNT) nanocomposites were synthesized via free radical polymerization of acrylamide, 2-acrylamido-2-methylpropane-1-sulfonic acid and acrylic acid in the presence of vinyltrimethoxysilane (VTMS) as the crosslinker.

The main objectives of this thesis are the preparation of mechanically improved SAP-HNT nanocomposites, which have higher swelling ratios and longer water retention capacities. The effect of HNT tubular shape nanofiller integration into the crosslinked polymer structure is investigated in order to observe the changes in the swelling- release performance and mechanical properties of SAPs.

2

To be able to design a super-absorbent polymer, which has the desired swelling and mechanical performance, the crosslink density of polymer should be tuned in a controlled manner since the swelling performance of SAPs changes inversely proportional to the crosslinking density. Therefore, in Chapter 4, the effects of molecular weight and mole amount of PEGDA crosslinker on the crosslink density of SAPs are investigated with the synthesis, characterization, and performance tests of SAPs. The crosslink densities of PEGDA-SAPs were calculated according to two different parameters, the chain length and mole amount of PEGDA crosslinker. Thus the correlation between crosslinker chain length, crosslinker amount, and swelling performance are demonstrated, respectively.

1.2. Thesis Outline

The rest of Chapter 1 includes detailed information about the synthesis and crosslinking mechanisms of SAPs. In Chapter 2, experimental steps of SAPs synthesis and SAP nanocomposites preparation, equilibrium swelling/release measurements, crosslinking density determinations are explained in detail. Later in Chapter 2, characterization methods of SAP nanocomposite and results of characterizations which demonstrate polymerization success, swelling/release kinetic of SAPs, and rheological behavior of SAP nanocomposites, are presented. In Chapter 3, firstly synthesis method and characterization results of the PEGDA crosslinker are provided in detail. Also, Chapter 3 comprises the synthesis methods, crosslinking density calculations, swelling/release performance test results, and characterization results of the PEGDA-SAPs.

1.3.Literature Review

1.3.1. Hydrogels and Super-absorbent Polymer Synthesis

SAPs are a special class of hydrogels with very high absorption capacities. While swelling or absorption capacity of hydrogels is up to 10 g/g, SAPS are able to swell and absorb water up to 600-1000 g/g [5, 14]. SAPs or hydrogels are not dissolved in water due to the crosslinked 3-dimensional polymer structure. When SAPs are immersed in an aqueous medium, the swollen polymer creates a gel by absorbing water, the water uptaken into the polymer network holds between the crosslinked points. The lightly crosslinked 3D polymer structure is procured with physically and/or chemically crosslinking of polymer chains. The swelling mechanism of SAPs are presented in Figure 1.1 [33]. The hydrophilic functional groups such as -OH, -COOH, -CONH-, -CHO, -COONa, -SO3H, -NH2 in the polymer chains contribute the absorption of water into the crosslinks between chains. In case of an ionic gel behavior, the osmotic pressure difference between the inside and outside of the gel will increase with the increase of dissociated sodium carboxylate groups concentration in the gel. Since the osmotic pressure difference is a driving force raising the swelling capacity of SAPs, the absorption capacity of SAPs increases with the osmotic pressure difference. The maximum swelling capacity is reached in the deionized water medium [25].
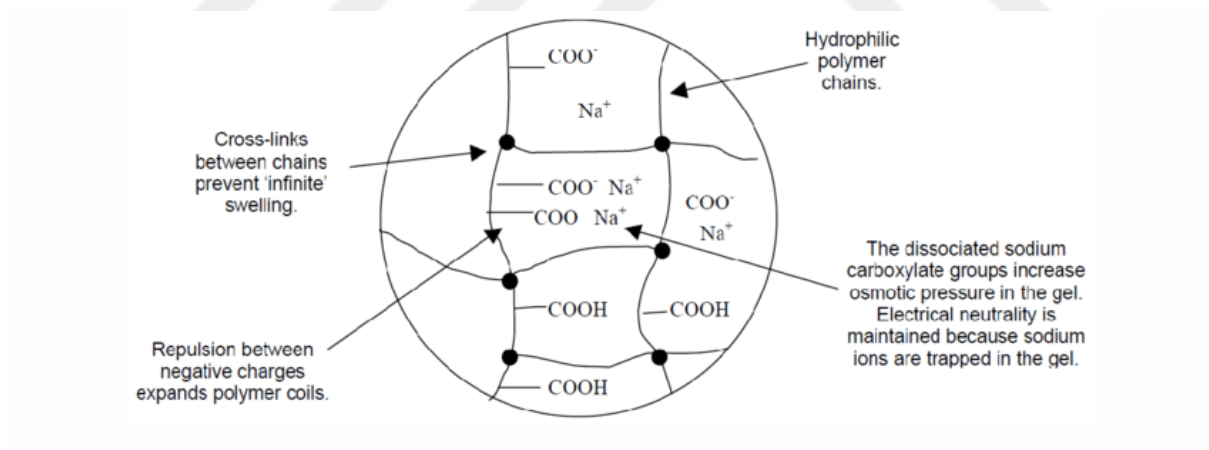
Figure 1.1 The swelling mechanism of super-absorbent polymers [34]

The synthesis procedures of hydrogels are mostly based on crosslinking polymerizations which can be physical or chemical process. To synthesis hydrogels via physical crosslinking different methods can be used such as ionic, hydrogen bonding crosslinking which are the results of temporal junctions, physical interactions, or polymer chain entanglements. Chemically crosslinking polymerizations of hydrogels can be categorized under three main polymerization methodologies; addition, condensation, and irradiation polymerizations. A

crosslinking agent are used in chemical crosslinking polymerization in order to provide covalent bonding between the polymer chains. The synthesis procedures of hydrogels via crosslinking polymerization are addressed under the head of crosslinking mechanisms of SAPs in more detail.

1.3.2. The Classification of SAPs

The different classifications of SAPs are listed in Figure 1.2 according to crosslinking, sources, electrical charge, physical appearance, degree of biodegradation, polymeric composition, responsive properties. The description of hydrogels based on preparation methods, sources and ionic charge are explained in detail.
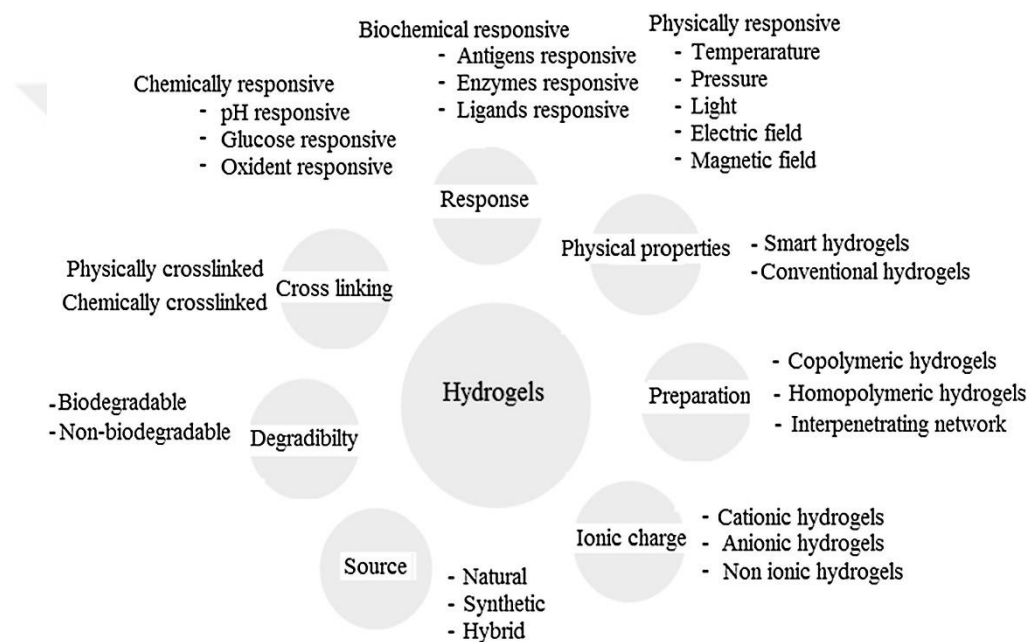
Figure 1.2 The classification of hydrogels according to different properties [35]

3 types of hydrogels are categorized based on polymer composition determined by polymer preparation method; homopolymeric, copolymeric and interpenetrating polymeric.

-   Homopolymeric hydrogels: The polymer network forms from repeating unit of a single monomer. Therefore, the properties of the crosslinked skeletal polymer structure depend on the basic structure of single monomer.

-   Copolymeric hydrogels: Two or more monomer species with at least one hydrophilic component are polymerized in order to obtain copolymeric hydrogels. Polymer network is determined by the arrangement of monomers as a random, block or alternating configuration.

- Interpenetrating network (IPN) polymeric hydrogels: Two polymer networks are combined in a network form, at least one polymer is synthesized or crosslinked in the presence of another polymer network. Pre-polymerized hydrogel is immersed into the polymerization solution of monomers, crosslinker and initiator. In this way, the interlocked structure is obtained by the combination of two different polymer networks. The combination of crosslinked and non-crosslinked polymer networks is described as semi-IPN hydrogels. [26]

SAPs are classified into two sections, natural and synthetic polymers based on their sources. Natural polymers consist of proteins, polysaccharides such as collagen, gelatin, agar, starch, and alginate. Acrylic based monomers used in chemical polymerization such as acrylamide, acrylic acid, methacrylic acid, vinyl alcohol form synthetic SAPs [26]. In the recent times, higher absorption capacity [25], more durable gel life [26] and higher mechanical strength [27] of synthetic SAPs make them more preferable than natural ones since they are more compatible for industrial production and utilization. In addition, combined SAPs can be prepared using both natural and synthetic polymers. [28] These are generally synthesized via graft polymerization. In this way, the limitations of synthetic hydrogel technology such as non-biodegradability, toxic effect of unreacted monomers and crosslinker are prevented with the combination of natural and synthetic polymers [35]. More ecofriendly SAPs are obtained with grafting natural and synthetic sources because combination of two sources provides more biodegradable SAPs [29].

SAPs are divided into 4 categories regarding to the presence or absence of electrical charge on the polymers network as follows:

- Non-ionic: Neutral crosslinked polymer network
- Ionic: Anionic or cationic crosslinked polymer chains
- Amphoteric electrolyte: Including both acidic and basic groups in crosslinked polymer chains.
- Zwitterionic: Including anionic and cationic groups together in repeating unit structure [26].

In ionic hydrogels, the driving force effect of osmotic pressure increase due to the ionic concentration difference between the inside and outside of the gel. Therefore, the swelling capacity of SAPs is improved with the presence of ionic groups in the crosslinked polymer chains [25].

Zwitterionic hydrogels contain both positive and negative ions in every monomeric unit of polymer chains. Therefore, mechanically strength, salt-tolerant hydrogels are prepared with the utilization of zwitterionic groups. Mostly, sulfobetaines, carboxybetaines and phosphorylbetaines monomers are used in order to synthesize zwitterionic betaine polymers. The most preferred monomer is sulfobetaine because of its economic price, easy accessibility, and commercial existence [36]. The swelling capacity of hydrogels in saltwater decreases due to the increasing ion concentration in the outside medium of gel. However, the utilization of zwitterionic monomers in SAPs backbone gives possess a high ion tolerance in saltwater thanks to the coexistence of the opposite charges in the crosslinked polymer chains [37].

1.3.3. The Crosslinking Mechanisms of SAPs

The crosslinks in the hydrophilic polymer chains are present to avoid the dissolution of polymer in an aqueous environment. The three-dimensional hydrogel network has been formed by chemical or physical crosslinking. The graphical representation of chemical and physical crosslinking mechanisms is illustrated in Figure 1.3 [38].
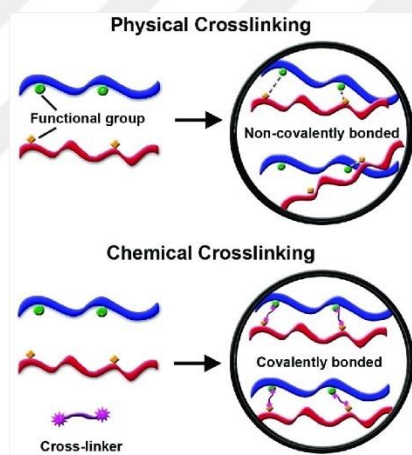
Figure 1.3 The graphical representation of physical and chemical crosslinking mechanisms [38]

The physical crosslinking is the results of temporal junctions, which arises from either physical interactions or polymer chain entanglements. Ionic interactions, hydrogen bonds and hydrophobic interactions are the different methods of physical crosslinking. Crosslinking agents, which are toxic compounds, are not used in physical crosslinking. The absence of any crosslinking agent makes the physical crosslinking procedure easy and convenient. The physically crosslinked gels can be applied directly without any requirement of removing/extracting toxic compounds such as crosslinkers [39]. The different methods used in physical crosslinking are listed below.

Freeze-thawing process: In this simple process, organic and bulk solvent or low molecular weight solutes are crystallized by freezing, the space between polymer chains decreases, and the polymer concentration increases. As a result, the polymer chains form a network, a consequence of the polymer chain alignment due to the force of increasing polymer concentration, and the hydrogen bonds and covalent interactions hold this joined network. Period of freeze-thawing, pH, freezing temperature, and time are the parameters that affect the degree of physical crosslinking. Natural materials, cellulose, and cellulose-derived materials are commonly used in the physical crosslinking process [40, 41]. Zhang et al. have studied the effect of freeze-thaw cycles on the compressive strength of PVA gel [42]. They demonstrate that the crosslink density of hydrogels increases with the increase of freeze-thaw processes because the intra- and intermolecular hydrogen bonds increase with multiple freeze-thaw cycles. As a result, this causes an enhancement of the compressive strength of hydrogels [42].

Crosslinking by Ionic Interaction:

The ionic interactions between two molecules of opposite charges or polyelectrolytes cause physical crosslinking and construct a crosslinked hydrogel polymer network. Polyelectrolyte complexes occur between the electrostatic interaction of macromolecules because of the opposite charges. For example, the natural polycationic biopolymer chitosan quickly generates polyelectrolyte complexes with anionic polyelectrolytes such as alginate, pectin. Also, some synthetic polymers such as polyacrylic acid and polyphosphoric acid can easily form polyelectrolyte complexes due to the electrostatic interactions between cationic amino groups of chitosan and anionic acid groups [43]. The mixing ratio and charge density of the polymers, environment of polymer solution are the factors that affect the generation of polyelectrolyte complexes and physically crosslinking hydrogel structure. The opposite electric charge groups of two polymers construct the physically crosslinked hydrogels via the electrostatic ionic interactions.

In chemical crosslinking consists of permanent junctions in other words i.e., covalent bonds between polymer chains provides crosslinking in the SAP structure. Chemical crosslinking can be categorized under three significant categories of methodologies:

1. Addition polymerization / Chain growth Polymerization: Similar to the free radical polymerization
    - Solution polymerization
    - Suspension polymerization

- Photo-polymerization

2. Condensation polymerization / Step Growth Polymerization

3. Irradiation Polymerization: High energy radiation / photo crosslinking

Surface crosslinking

Bulk or core crosslinking (Self-crosslinking): The crosslinker is inserted into the polymer backbone as a monomer. Also called bulk crosslinkers, these agents are bifunctional or multifunctional monomers possessing one or more unsaturated bonds in their chemical structure and are usually chemically more active than other monomers [44]. In that sense, alkoxysilanes, having both organic and inorganic functional groups, are characterized as multifunctional bulk crosslinkers as they are able to form multiple covalent bonds between inorganic and/or organic species [45, 46].

Crosslinking density calculation

The most widely used method for crosslink density calculation of polymer networks is the Flory-Rehner model [47]. The number of crosslinked sites or the molecular weight between crosslinks is a primary parameter to calculate the crosslink density of polymer networks. The polymer is swollen in a solvent to calculate the molecular weight of polymer chains between two consecutive junctions. Schweitzer et al. have investigated the crosslinking density determination of a silicone elastomer [48]. They used the Flory-Rehner model to calculate the crosslinking density of elastomers, and the molecular weight between crosslinks M_c is calculated formula below

$$M_c = -\frac{\rho_e V_s \left(\phi^{1/3} - \frac{2\phi}{f} \right)}{\ln(1 - \phi) + \phi + \chi\phi^2}$$

Figure 1.4 The formula for calculation of molecular weight between crosslinks [48]

Here ρ_e is the density of the dry polymer, V_s the molar volume of the solvent (in $cm^3 mol^{-1}$), φ the polymer volume fraction, f the functionality of the crosslink, φ_n the polymer network fraction in the swollen network, and χ the Flory-Huggins polymer-solvent interaction parameter. The equation above relates the capacity of solvent uptake while swelling a polymer in a solvent by calculating the molecular weight per crosslink unit.

The formula below defines the polymer volume fraction, φ in the swollen equilibrium state as

$$\phi = \frac{(m_0 - m_0 f_{\text{silica}})/\rho_e}{(m_0 - m_0 f_{\text{silica}})/\rho_e + (m - m_0)/\rho_s}$$

Figure 1.5 The polymer volume fraction, φ calculation formula in the swollen equilibrium state [48]

The Flory-Huggins polymer-solvent interaction parameter is calculated with the formula below

$$\chi = \frac{V_m(\delta_e - \delta_s)^2}{RT}$$

Figure 1.6 The Flory-Huggins polymer-solvent interaction parameter formula [48]

The affinity between the polymer and solvent is stated with the solubility parameter or Hildrebrand solubility parameter δ (in cal1/2 cm−3/2). The crosslinked polymer swell effectively when the solubility parameter, δ similar to the solubility parameter of solvent. Here V_m is the molar volume of polymer; δe and δs are the Hildebrand solubility parameters (in $cal^{1/2}\ cm^{-3/2}$) of the polymer and solvent, respectively; R is the gas constant, and T is the temperature (with RT = 580 cal mol^{-1} at 20 °C).

Finally, after calculating the molecular weight between crosslinks, M_c, the crosslink density of polymer networks is calculated with the formula below

$$\nu = \frac{\rho_e}{M_c}$$

Figure 1.7 The formula for calculating the crosslink density of polymer network [48]

The formula above defines the relation between Mc and crosslinking density. As the molecular weight of polymer chains between crosslink points decreases, the crosslinking density increases.

1.3.4. Application areas of SAPs

SAPs in Agriculture

The utilization of SAPs in agriculture comes into prominence day by day due to the rising need for smart agricultural solutions. SAPs are mainly used as water reservoirs under soil for plants [49]. The unique swelling and retaining characteristics of super-absorbent polymers make them suitable for agricultural applications. Water is one of the essential parameters in

plant growth to be able to feed plants by nutritive elements [50]. On the other hand, global warming and climate change cause irregularities in rainfall patterns resulting in long-term drought in many agricultural lands. Therefore, limited water sources should be used efficiently to overcome water shortages. Yet, the traditional manual irrigation systems in agriculture cause inefficient use, resulting in contamination of natural resources and water loss. Today, 70% percent of freshwater in the global is consumed in agriculture and this critical amount illustrates that intelligent agricultural products will be an effective solution for sustainable agriculture by providing less water use [51, 52]. In this sense, SAPs offer smart solutions to overcome the indiscriminate consumption of water in agricultural irrigation.

Majority of literature examples deal with the effect of SAPs on soil moisture, plant growth and seedling and indicate that the presence of SAPs near the plant roots increase the water absorption and retention capacity of soil, improve the plant quality [53]. In addition, the irrigation frequency and excess water use are reduced by the utilization of hydrogels [54]. Moreover, SAPs enable agriculture in areas under drought stress due to their water holding capacity [55]. Once SAPs are placed under the soil near the roots, they supply the water demand of plants by releasing water with the osmatic pressure difference [56]. Mixing super-absorbent polymers with soil increase the physical properties of soil, plant yield and seed germination [57].

In addition to providing better water management in soil, fertilizers have been loaded to super-absorbent polymers for use as nutrient carriers for plants[58]. Recent experimental studies have presented that fertilizer retention in the soil is increased through the implementation of fertilizers together with super-absorbent polymers [59]. In another study, it was focused on the membrane encapsulation technique of fertilizers with super-absorbent polymers in order to improve the utilization of fertilizers, and a slow release of fertilizers was provided with the encapsulation technique [60].

A superabsorbent-fertilizer composite is used as a controlled release system for raising the nutrient and water use efficiency. Hydrogels hold the fertilizer tightly inside. Therefore, the leaching of nutrients to the soil is reduced, and nutrient elements released with water can be directly taken by the plant root [53, 54, 56].

SAPs in Tissue Engineering

Biodegradable natural hydrogels have been considered as promising biomaterials in tissue engineering applications due to their biocompatibility, mechanical-biological properties,

11

hydrophilic nature, controlled degradation profile [61]. Hydrogels exhibit a suitable environment for faster cell growth to form the three-dimensional tissue scaffolds because they have the ability to swelling and holding high amounts of water, the possibility of diffusion of various substances, physical and biological tunability [62]. Biosynthetic hybrid hydrogels, involving both synthetic and natural polymers in their structure, are favored materials in scaffolds due to their biomechanical stability and controllable degradation profile. To synthesis enhanced biosynthetic hybrid hydrogels for cardiac tissue engineering applications, the graft polymerization of natural polysaccharide alginate and synthetic polyester polypropylene fumarate were carried out and obtained an enhanced hydrogel with a long-term cellular growth [61].

SAPs in Drug Delivery

Natural hydrogels such as collagen, chitosan, alginate are favored materials for drug protection and delivery due to their unique physical properties providing long-term continuous drug release. Since the releasing drug content in suited rate into the desired location in the body, hydrogel-based drug delivery systems develop the effectiveness of drug release by decreasing dosing intervals with a sustained release [63]. Temperature and pH sensitive hydrogels exhibit a controllable reversible swelling – deswelling behavior by changing the temperature or pH stimulus of the environment [64]. Zhang et al. prepared thermally sensitive semi-interpenetrating network hydrogel by radical polymerization of poly(N-isopropyl acrylamide) and β-cyclodextrin-grafted polyethyleneimine. As the environment temperature elevates above the lower critical temperature, thermally sensitive hydrogel exhibits a sustained drug release due to faster-shrinking kinetics. A prolonged drug release was observed with interpenetrating network thermally sensitive hydrogel [65].

This thesis aims to explain the relationship between mechanical properties and water retention capacity and the correlation between swelling ratios and crosslinking density. Therefore SAP nanocomposites with enhanced water retention capacities and SAPs with tunable crosslinking densities were synthesized, respectively. The synthesized SAP nanocomposites were structurally, thermally, and rheologically characterized with FTIR, TGA, and rheometer, respectively. Also, the crosslinking densities of SAP nanocomposites were calculated and compared with swelling performance tests to observe the correlation between crosslink density and swelling capacities. Finally, the mechanical properties of SAP nanocomposites were performed via rheology results to see the enhancement in swelling-release kinetics. Improving mechanical properties and water retention capacities of SAP nanocomposites are

fundamental aims since the SAP nanocomposites were synthesized intended for agriculture applications.

On the other hand, the correlation between crosslink density and swelling capacities was confirmed by preparing the SAPs with tunable crosslink densities. Therefore, to eliminate the influencing factors such as nanofiller (HNT), crosslinker type (self-crosslinking) on crosslink density, different crosslinkers were synthesized to prepare SAPs with tunable crosslink densities. Then the effect of crosslinker chain length and crosslinker amount on crosslink density were analyzed.

The obtained results are significant to clarify the effect of nanofiller addition on mechanical properties and swelling-release capacities. In addition, the tunable crosslink density mechanism of SAPs was explained via the correlation between crosslinker chains length, amount, and crosslink density
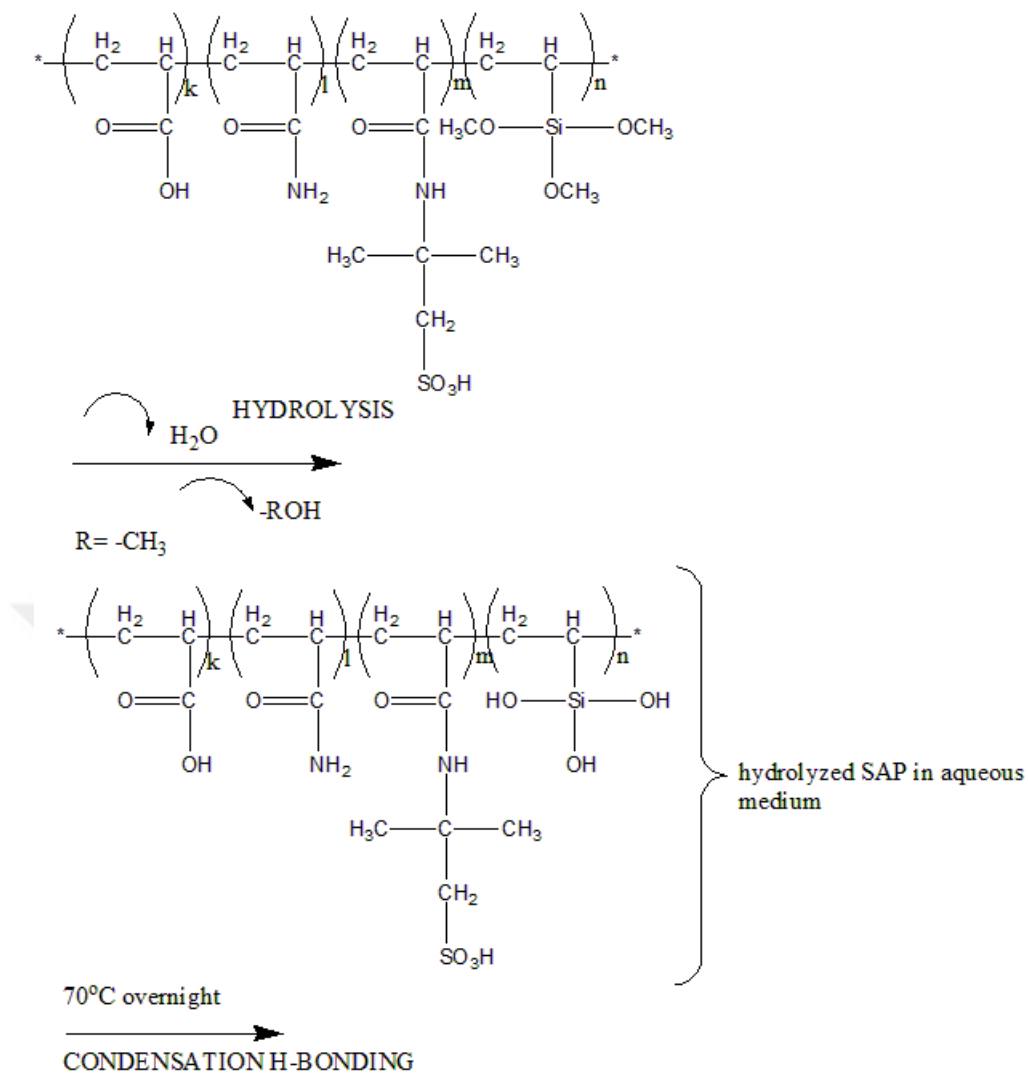
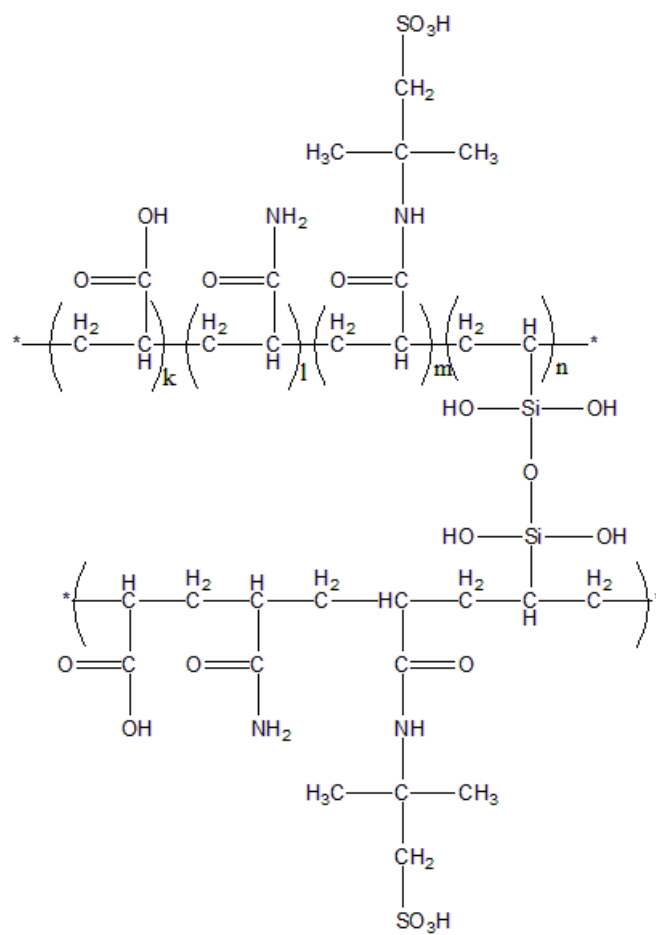**Chapter 2**

2. Experimental Methodology

2.1. Materials

Acrylamide (AM, ≥99% HPLC) and 2-acrylamido-2-methylpropane-1-sulfonic acid (AMPS, ≥99%) monomers were purchased from Sigma Aldrich and used without any further purification. Acrylic acid (AA, analytical grade) was purchased from Alfa Aesar and used as received. Initiator ammonium persulfate (APS, ≥99%) and crosslinker vinyltrimethoxysilane (VMTS, 98%) were obtained from Sigma Aldrich. Sodium hydroxide solution 10 mole/L and ethanol (EtOH, absolute-99.9%) were purchased from Merck and used without further purification. Halloysite nanotubes (HNT) was kindly provided by ESAN. All solutions were prepared with distilled water.

2.2. Super-absorbent Polymer Synthesis

SAP was prepared via free-radical polymerization in deionized water. The random copolymer was synthesized from acrylic acid (AA), acrylamide (AM) and 2-acrylamido-2-methylpropane-1-sulfonic acid (AMPS) monomers using ammonium persulfate (APS) as the free radical initiator, in the presence of vinyltrimethoxysilane (VTMS) as the crosslinking agent. An amount of AM and AMPS were dissolved in water and then AA was added into the solution mixture. After complete mixing took place and a clear solution was obtained, the highly acidic monomer solution, due to the acrylic acid, was neutralized by 12 M sodium hydroxide to adjust pH to 8. Thereafter, monomer solution was transferred into a three necked flask connected to a condenser apparatus and purged with Nitrogen to remove excess oxygen present in reaction environment. After the mixture was bubbled with Nitrogen gas for 15 minutes, VTMS was added to the mixture under vigorous mixing. The mixture was subjected to further mixing and bubbling for an extra 15 minutes to remove any excess oxygen and air from reaction medium. In another flask, APS free radical initiator was dissolved in water and then added to the reaction mixture. The polymerization was carried out under reflux at 78 °C in an oil bath for 2 hours. The amounts of monomers used in SAP synthesis are given in Table 2.1.

A transparent viscous polymer solution was obtained at the end of the reaction. The three-necked flask was then taken out from the oil bath and polymer solution was cooled down to room temperature. Finally, the resulting polymer was precipitated in ethanol in the form of white powder. The super absorbent polymer was then dried at 70 °C for 2 days.

HYDROLYSIS

H_2O

-ROH

R= -CH_3

hydrolyzed SAP in aqueous medium

70°C overnight

CONDENSATION H-BONDING

15

Figure 2.1 The reaction and crosslinking mechanism of SAP2HNT0

2.3. SAP- HNT Nanocomposite Preparation

After the monomer solution was prepared and pH adjusted to 8 with 10 M NaOH, an amount of HNT was added to the monomer solution. Then, the polymerization process was continued as in the SAP synthesis. First, VTMS was added to the inert reaction medium. The initiator was then added to the reaction mixture, and polymerization was carried out at 78 °C for 2 hours. When the polymerization was finished, an opaque viscous polymer solution was obtained for the precipitation in ethanol. The precipitated polymer powder was then dried at 70°C or 2 days. The amounts of HNT and monomers used in SAP-HNT nanocomposite synthesis are given in Table 2.1.

Table 2.1 The amounts of monomers and HNT used in SAP and SAP-HNT nanocomposite synthesis

Eq. Mole	AM	AMPS	AA	VTMS	HNT Amount, %
SAP2HNT0	0.06	0.005	0.07	0.001	0

SAP2HNT1	0.06	0.005	0.07	0.001	1
SAP2HNT5	0.06	0.005	0.07	0.001	5
SAP2HNT7	0.06	0.005	0.07	0.001	7
SAP2HNT9	0.06	0.005	0.07	0.001	9

2.4. Equilibrium Swelling Measurement of SAP and SAP- HNT Nanocomposites

The dried powder SAP and SAP-HNT nanocomposite samples are weighted before swelling in a distilled. The swollen hydrogel was weighed in a periodic interval by filtering out from the water to calculate the ESR value. The equilibrium swelling ratio (ESR) is calculated according to Eq (1):

$$ESR(g/g) = \frac{W_s - W_d}{Wd} \quad (1)$$

Equation 1 The equilibrium swelling ratio formula

where W_s is the weight of hydrogel at equilibrium and W_d is the weight of the dry polymer.

The water release ratios were calculated with the same equation (Eq 1); only the ESR mark was changed to EShR to emphasize the contrast between swelling and release ratios.

2.5. Crosslink Density Calculation of SAPs

The ratios of crosslinked points of hydrogels could not be determined with Nuclear Magnetic Resonance Spectroscopy (NMR) since the super-absorbent polymers were not dissolved in any solvent, only swollen in water. However, the number of crosslinked points determines the equilibrium swelling ratio values because the maximum swelling capability depends on the average molecular weight between crosslinked points. Therefore, the determination of crosslinking density through the average molecular weight between crosslinked points is required to clarify the swelling capacities of SAPs.

Hence, the crosslinking density and the average molecular weight between crosslinks were calculated by Flory-Rehner's Theory of Swelling [66]. The average molecular weight between crosslinks is calculated by the equation 2 [67]:

$$\overline{M_c} = \frac{-\rho V_s V_r^{1/3}}{\ln(1 - V_r) + V_r + \chi V_r^2} \quad (2)$$

Equation 2 The formula of average molecular weight between crosslinks

17

Where V_s and V_r denote the molar volume of solvent (18 g cm^{-3}) and volume fraction of the SAP in swollen polymer, respectively. ρ stands for the density of dry SAP and χ is the Flory-Huggins interaction parameter calculated from;

$$\chi = \frac{V_1(\delta_2 - \delta_1)^2}{RT} \quad (3)$$

Equation 3 Flory-Huggins interaction parameter

Here, V_1 denotes the molar volume of the solvent and $\delta_2 - \delta_1$ states the Hildebrand solubility parameters (cal$^{1/2}$ cm$^{-3/2}$) for water and SAP, respectively. Once M_C is obtained from Eq. 2, the crosslinking density is calculated by;

$$\nu = \frac{\rho_{SAP}}{M_c}$$

Equation 4 Crosslink density formula [68]

2.6. Characterization of SAPs

- ATR/ FTIR Spectroscopy

Synthesized SAP and SAP-HNT samples were characterized by Attenuated Total Reflectance Fourier Transformed Infrared Spectroscopy (FTIR) collected on a Thermo Scientific iS10 ATR-FTIR spectrometer from 550 to 4000 cm−1, with a resolution of 0.5 cm−1. A total of 32 scans were gathered and baseline corrected.

- Thermo Gravimetric Analysis (TGA)

Thermal behavior of powder SAP and SAP-HNT samples were characterized by a Netzsch STA (Simultaneous Thermal Analysis) 449 C Jupiter differential thermogravimetric analyzer with 50 mL/min flow from 30 to 1000 °C at a linear heating rate of 10 °C/min under N$_2$ atmosphere.

- Gel Permeation Chromatography (GPC)

The molecular weight of non-crosslinked SAP was determined by using Malvern Panalytical's OMNISEC Gel Permeation Chromatography (GPC) device with a light scattering detector. The non-crosslinked polymer was dissolved in water at 35°C. The flow rate was 0.7 mL/min, the injected volume was 100 µL, and the sample concentration was 1 mg/mL.

- Density

The density of SAP and SAP-HNT nanocomposites was determined using Quantachrome Ultrapyc 1200e Automatic Gas Pycnometer. The type of gas used is Helium, and purge flow is 1 min.

-Rheometer

The rheological behavior of synthesized polymers were characterized by an Anton Paar-Physica oscillatory rheometer (MCR 702 TwinDrive). The rheological measurements were performed at 25°C with a parallel plate (plate diameter of 25 mm, gap of 1 mm). All synthesized polymers in SAP2 data set were swollen in distilled water for 24 hours for rheology measurements. A strain sweep test was performed in order to determine test conditions in the linear viscoelastic (LVE) range. The shear strain value in the LVE range was determined at 6.2 Hz frequency and 0.01% amplitude gamma.

Chapter 3

3.   Results and Discussion

3.1. Structural Characterizations

3.1.1.   FTIR Spectral Analysis

Since the crosslinked SAPs are not able to be characterized by using NMR, the polymer structure of SAPs was confirmed via FTIR analysis. The FTIR spectra of synthesized SAP2 polymer set in Figure 3.1 shows that AM, AA, AMPS monomers and VTMS crosslinker have appeared in the polymer backbone.

The peaks at 1190 and 1040 cm^{-1} correspond to the stretching vibrations of -Si-O- and Si-O-Si in the VTMS structure. The broad peak between 3339.20 and 2985.88 cm^{-1} wavelength is ascribed to the vibration of -OH in AM, AA, AMPS and VTMS. The peak at 3339.20 cm^{-1} is due to the streching vibration of N-H in AM. The peak at 2934.88 cm^{-1} is attributed to the stretching vibration peak of -CH at the polymer backbone. The streching vibration peak of -C=O in AM, AA and AMPS structure is observed at 1650.88 cm^{-1}. The peaks at 1447 and 1411 cm^{-1} are due to the stretching vibrations of -C-N and -NH_2 in the acrylamide chemical structure. The peak at 1190 cm^{-1} is corresponded to the sulfone groups in the AMPS chemical structure.

In the FTIR spectra of SAP2HNT7and SAP2HNT9, the peak at 2360.83 cm^{-1} is probably just related to the background CO_2 in the spectrometer. The absorption by carbon dioxide (CO_2) in the environment may be observed near 2350 cm^{-1} since the purging with nitrogen was not performed enough [69].

The FTIR spectra of synthesized polymers consisting HNT are presented in Figure 3.1. The vibration peaks of -Si-O-, Si-OH at 1100-1050 cm^{-1} confirm the presence of HNT in the polymer structure.

According to FTIR results, the polymerization was carried out with the participation of all monomers, and the presence of HNT in the polymer structure was confirmed.
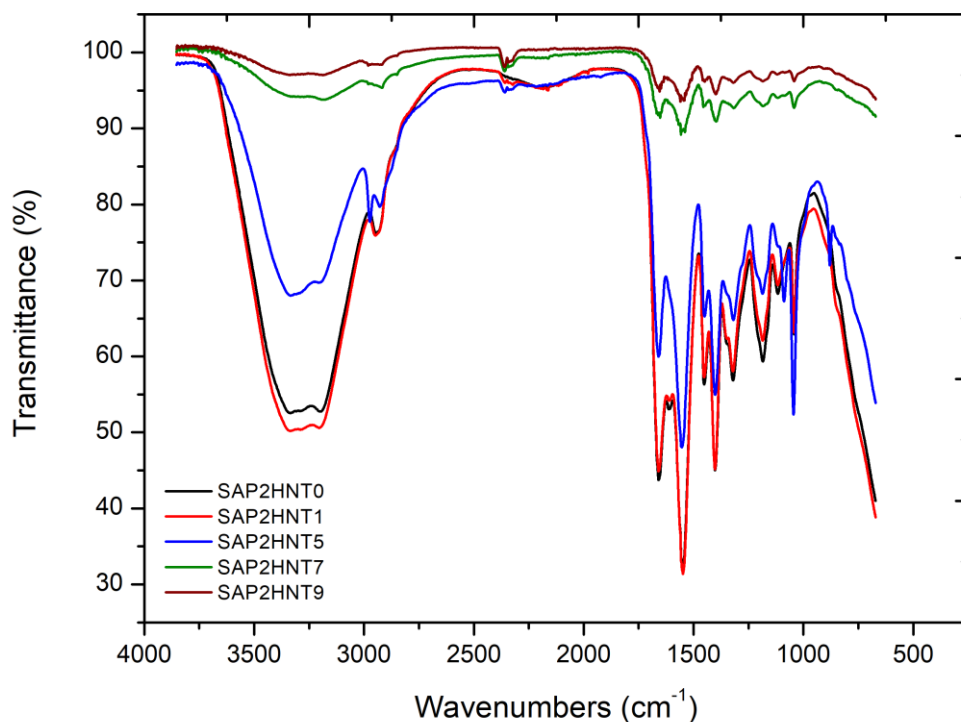
Figure 3.1 FTIR results of SAP2 polymers experiment sets

3.2.Thermal Characterizations

TGA Results of Synthesized SAPs

Thermogravimetric analysis results of SAP and SAP-HNT nanocomposites are presented in Figure 3.2. The trio-random copolymer structure of SAPs and 0, 1, 5, 7 % of HNT addition in SAP nanocomposite structure are verified in TGA results. 15% mass loss between 50-200°C stems from water loss in the polymer structure. AM and AMPS monomers in polymer structure degrade at 200-300°C. After 300°C, the sulphonic groups in the polymer chain start to degrade. The residual mass in nanocomposites, containing 0, 1, 5, 7 HNT, is 12, 14, 17, 19, respectively, demonstrating a 2% residual mass increase due to the HNT addition. TGA results confirm thermal properties of SAPs are enhanced with HNT addition, and the residual mass of polymer increased in direct proportion to the HNT amount.
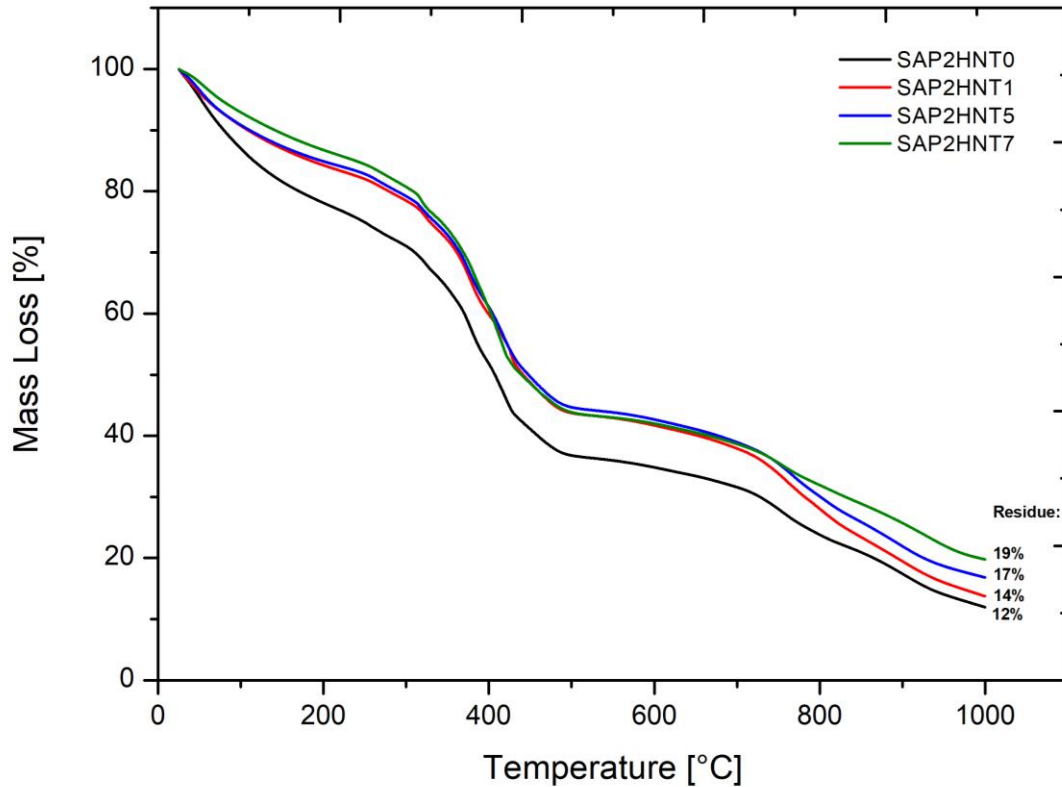
Figure 3.2 Thermogravimetric analysis of SAP and SAP-HNT nanocomposites

3.3.Swelling Behavior of Synthesized SAPs

SAP2 data set consists of 5 different polymers with 0, 1, 5 ,7 and 9% HNT amount. It is shown in Figure 3.3-a, addition of 5% HNT provides the maximum swelling, the swelling ratios decrease in 7-9% HNT amounts. Figure 3.3-b presents the slowest water release was obtained in 28 days with SAP2HNT1 polymer containing 1% HNT. The release graph (fig 3.3-b) shows after the 10th day, the water amount contained in the polymer structure significantly increase in SAP2HNT1. It means 1% HNT addition provides a more sustained water release regarding 5, 7 and 9% HNT addition.
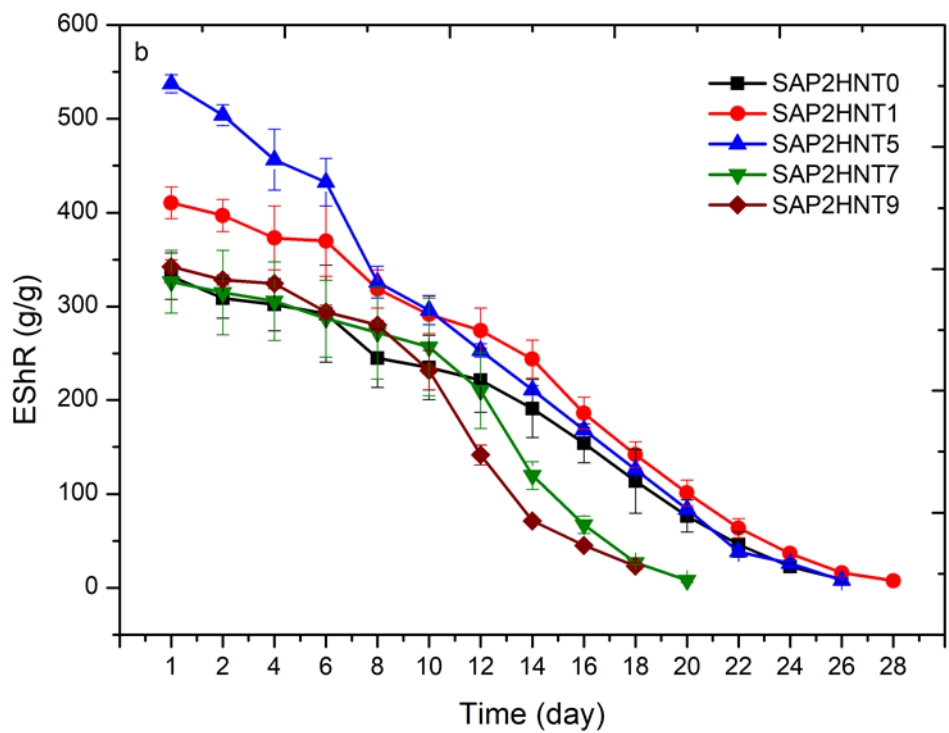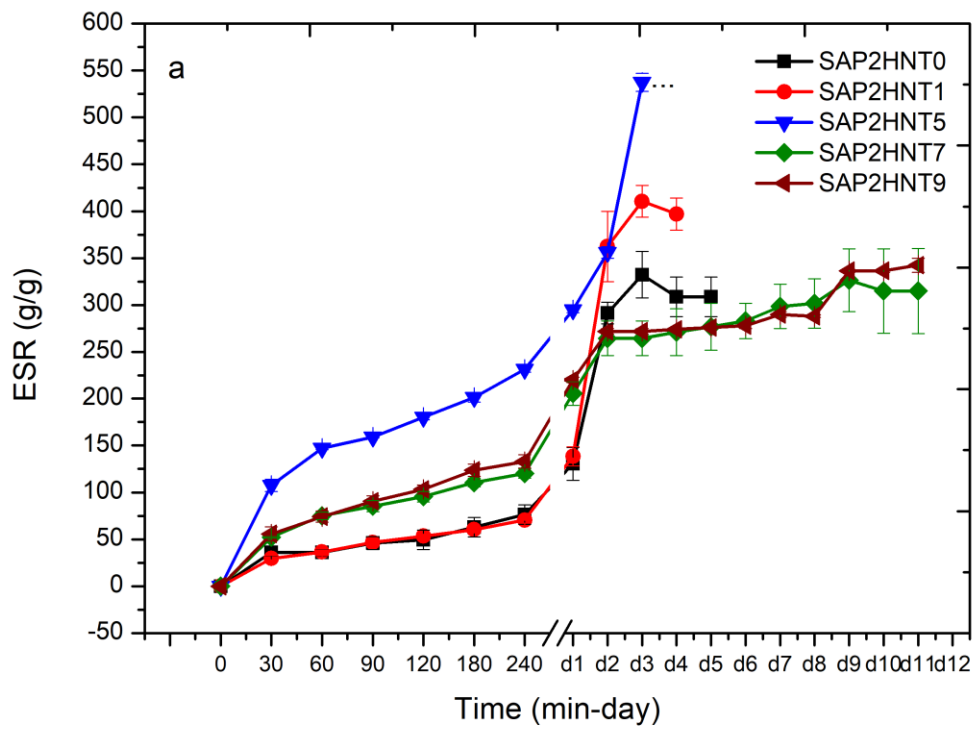
Figure 3.3 The swelling (a) and water-release (b) test results of SAP2 polymer set involving different amounts of HNT

The maximum swelling ratios in SAP2 dataset corresponding to HNT amounts are shown in Figure 3.4a. SAP2HNT5 with the addition of 5% HNT reached the maximum swelling ratio with a 537 g/g value.

The swelling kinetics of SAP2 dataset confirm the highest swelling value was observed in 5% HNT ratio and all nanocomposite polymers in the dataset swell 300-500 times of their weight and release the water in their structure for an average of 1 month.

3.4. Molecular Weight, Density and Crosslink Density Determinations

To determine the molecular weight of SAPs, the obtained polymer should be dissolved in a solvent. Since the crosslinked SAPs cannot be dissolved in any solvent, SAP polymerization was carried out without crosslinker addition. The obtained polymer was characterized by using gel permeation chromatography (GPC). The molecular weight of trio-random non-crosslinked polymer is presented in Table 3.1. Polydispersity index (PDI) value, equal to Mw/Mn, is 1.276, showing a low polymer chains length distribution.

As the density value of SAP is necessary for crosslinking density calculation, density of SAP and SAP-HNT nanocomposites were measured by using gas pycnometer. Table 3.1 shows the density of SAPs increase, as the HNT amount of SAP-nanocomposites increase, except for SAP2HNT5. The reason for this unexpected difference in SAP2HNT5 arises from the inserted HNT in reaction solution not completely participate to polymer structure, partially aggregate in the polymer matrix.

Table 3.1 Molecular weight of non-crosslinked SAP and density values of SAP and SAP-HNT nanocomposites

Molecular Weight of non-crosslinked SAP		Density of SAP and SAP-HNT Nanocomposites (g/cc)	
Mn – (Daltons)	940.971	SAP2HNT0	1.3936
Mw – (Daltons)	1,200 e 6	SAP2HNT1	1.6107
Mz – (Daltons)	1,399 e 6	SAP2HNT5	1.5266
Mp – (Daltons)	1.419 e 6	SAP2HNT7	1.6991
Mw / Mn (PDI)	1.276	SAP2HNT9	1.7198

Swelling experiments are a useful method to determine the crosslink density of network structures. Measured density (ρ_{SAP}) values are presented in Table 3.2, and $\rho_S = 1.0$ for our SAP dataset, and the m_0 is set as 0.2 g for all swelling experiments. The Hildebrand solubility parameter of SAPs are determined as 1.49 and 0.086 $(kJ\ cm^3)^{0.5}$ for water and SAP (set to poly (ethyl acrylate))[68], respectively.
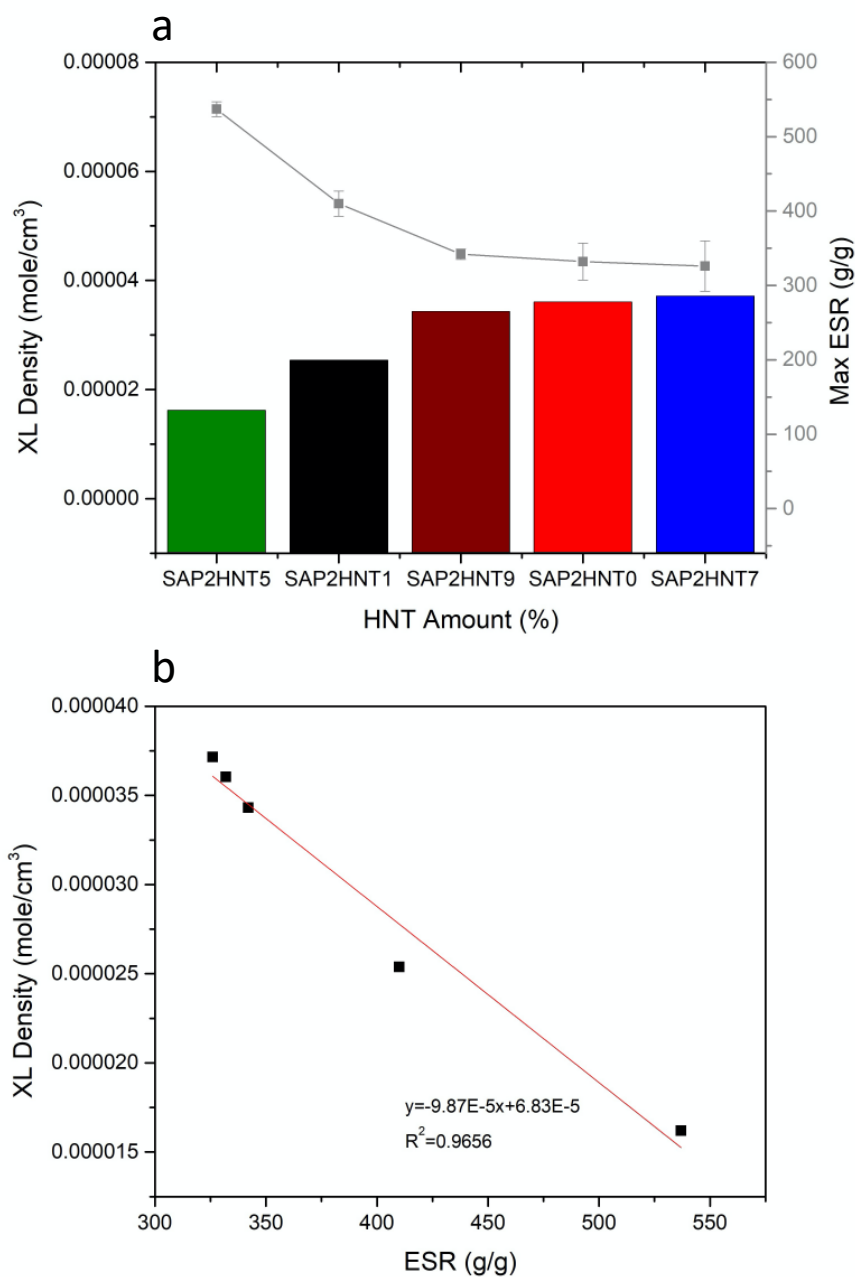
Figure 3.4 Maximum swelling ratios of SAP2 dataset polymers in water (a), crosslink density as a function of ESR (b).

Calculating XL density from the swelling experiments, we demonstrate the linear correlation between swelling and crosslink density. Furthermore, the inverse proportion between XL and ESR reveals the dependence of proposes that, although the HNT filler present in the SAP structure alters the maximum swelling capacities of SAPs (Fig 3.4-a), the XL density is still proportional to the molar volume of SAP in the nanocomposite structure (Fig 3.4-b). This means that the swelling is governed by XL density, which is an intrinsic property of synthesized SAPs.

3.5. Rheological Behavior of Synthesized SAPs

When SAP2 data set was analyzed to see the effect of HNT amount on storage modulus, it was observed the highest storage modulus value belongs to the SAP2HNT1 nanocomposite synthesized in the presence of 1% HNT (Figure 3.6). The storage modulus value decreases in between 5-7% HNT range while increasing in the presence of 1% HNT. The storage modulus values in between 5-7% HNT range is even lower than SAP2 polymers without HNT. This situation shows increasing HNT ratios cannot disperse in the gel matrix homogeneously and generate small aggregations confined into the gel matrix. On the other side, there is a relative increase in the storage modulus values with the increasing HNT amount (9%). It means that the addition of higher amounts of HNT increases the aggregate diameter and leads to a decrease in the integration between aggregate and gel matrix.

As a result, when all rheology measurement results are discussed, storage modulus values in the SAP2 data set have higher values due to the large amounts of AA monomer in the polymer structure, and the maximum storage modulus value is reached with the addition of 1% HNT. The non-monotonous trend in G' is governed by the three different of HNT incorporation into nanocomposite structure (Figure 3.5). In the first mechanism, the HNT molecules participate into nanocomposite structure via secondary interactions. The sharp increase observed in SAP2HNT1 suggests that small amounts of HNT (around 1 wt%) introduced into SAP structure makes a positive impact on G'. This can be explained by additional intermolecular interactions formed between HNT and SAP structure, which may act as physical crosslinking sites and/or entanglement points[67]. In the second mechanism, As the amount of HNT introduced into SAP structure is increased between 1-7 wt%, the storage modulus drops because HNT alters crosslinking mechanism of SAP by providing additional binding sites to silane crosslinker. This gives rise to a competition between self-crosslinking of SAP polymer chains and SAP grafting onto HNT surface. The more SAP is grafted on HNT surface, the looser and the less crosslinked the gel becomes, and eventually

results in lowered storage modulus[70]. And finally in the third mechanism, once a certain amount of HNT is introduced into nanocomposite structure (>7 wt%), the probability of individual HNT molecules find each other increases, thus intra-molecular interactions between HNT-HNT molecules becomes the preferred mechanism of interaction for HNTs. This results in HNT agglomerates in SAP nanocomposite, which gives rise to fewer interfacial interactions between HNT and SAP molecules eventually fluctuates the storage modulus[71]. As the gel structures undergoes to repeating destruction, reconstruction and agglomeration processes under constant shear[72], fluctuated shear responses are observed, particularly after 5% HNT incorporation.
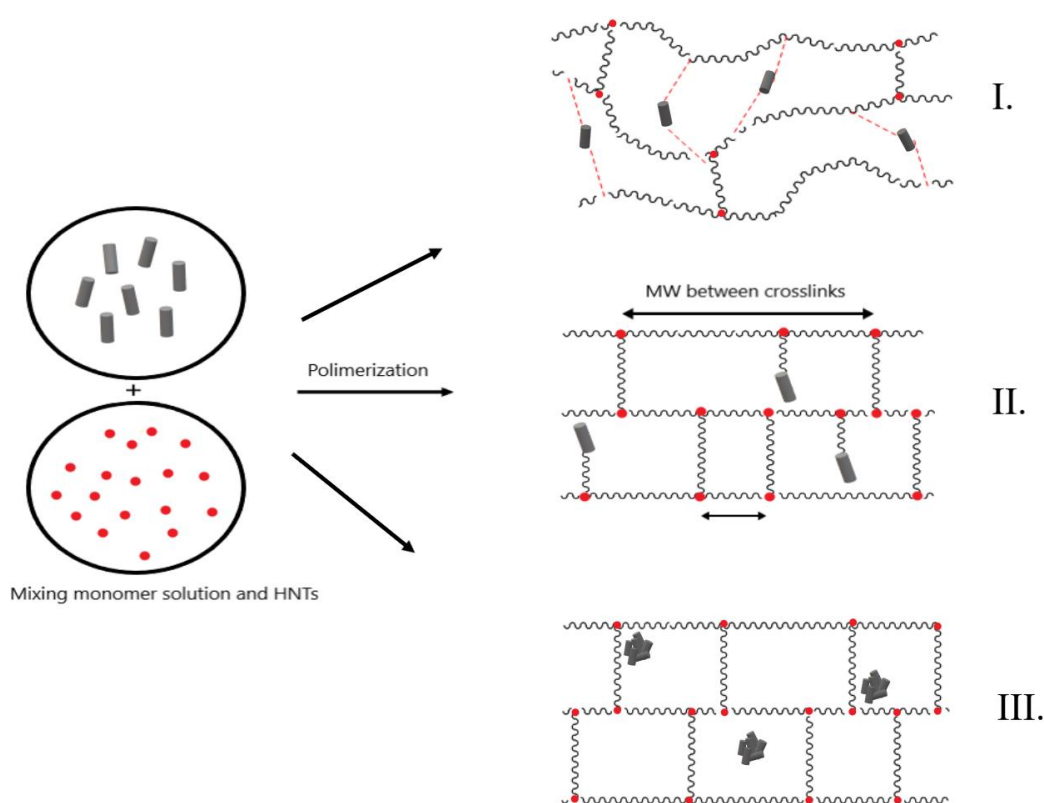
Figure 3.5 The graphical representation of three different HNT incorporation mechanisms into SAP nanocomposite structure

As explained in the first mechanism, the maximum storage modulus was reached in SAP2HN1 with 1% HNT addition due to the physical crosslinking through intermolecular interaction between HNT and SAP structure. The increase in the storage modulus correlates with the water release time of SAP2HN1. Figure 3.3-b presents the longest release period was

observed in SAP2HNT1. This correlation was confirmed with the obtained maximum storage modulus with 1% HNT addition and the enhancement in water release time of SAP2HNT1.
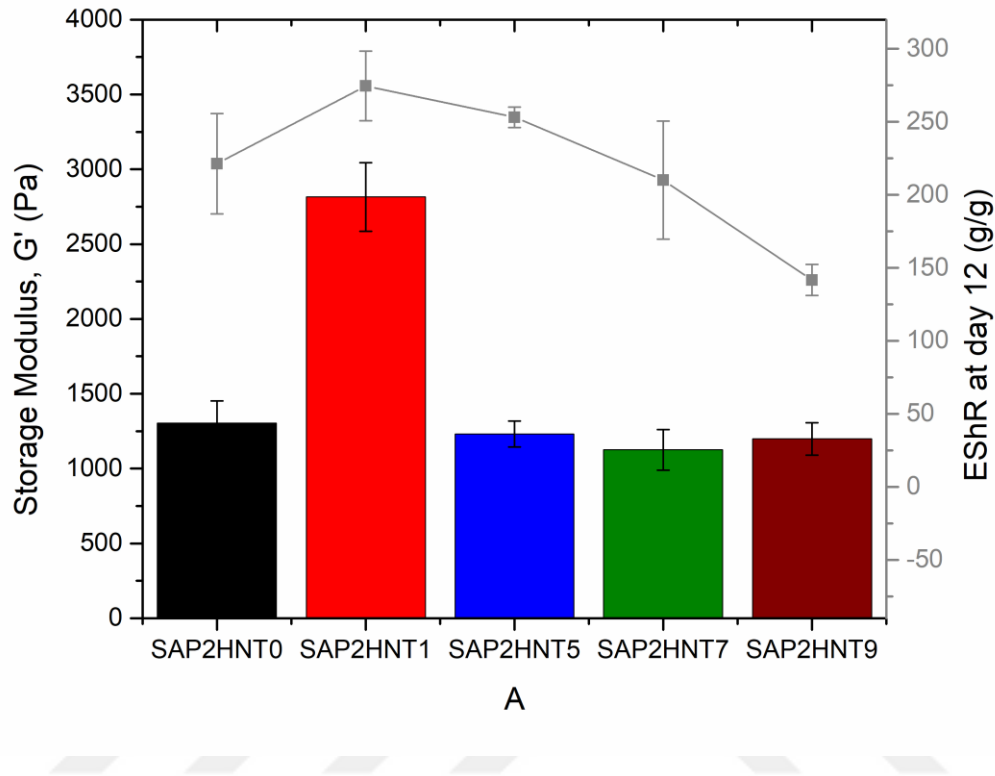
Figure 3.6 Storage modulus results of SAP and SAP-HNT Nanocomposites

3.6.Application of SAP2HNT5 on Different Types of Soils

In order to observe the effect of Soygel on different soil types, an experimental setup was prepared in three different soil types, sandy, loamy, and clay soils, with 0.5% and 5% SAP by weight and the control group at three different doses. First, soil water saturation capacities of sandy, loamy, and clay soil types were determined by calculating the amount of water given. After weighing equal amounts, 60 g of 3 different soil types, the maximum soil water capacities were calculated as 18, 33, and 33 mL for sandy, loamy, and clay soil, respectively. The experimental setup, in Figure 3.7-a was prepared with four repetitions of control, 0.5% and 5% SAP doses for three different soil types. The moisture measurement probe is immersed in the soil, and the soil moisture level is measured in the range of 1-10 values (Figure 3.7-b)
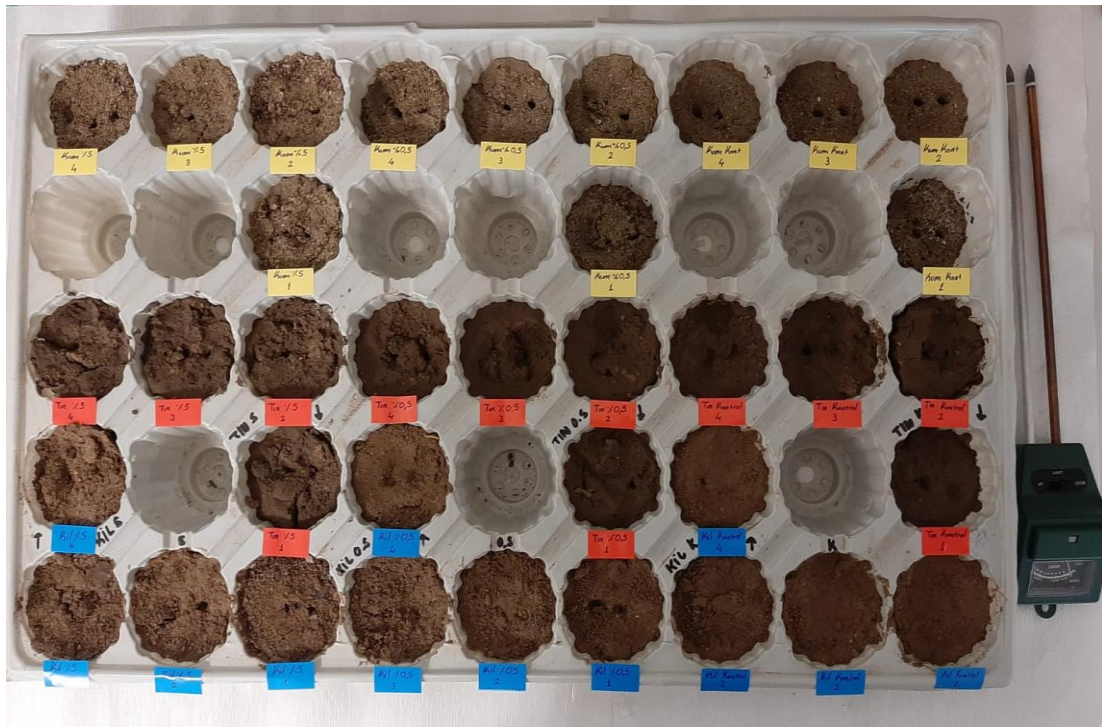
Figure 3.7 The experimental setup of loamy, clay, and sandy soil with control, 0.5% and 5% SAP doses(a) and procedure of soil moisture measurement with moisture probe (b)

In the first three days, the SAPs in the soil were irrigated with the amount of water calculated according to 80% of the maximum soil water holding capacity. As a result, the soil moisture level with control and SAP groups reached their maximum value, and SAPs in the soil

achieved the maximum swelling capacity. At the end of the 3rd day, irrigation was stopped, and only the soil moisture level was measured.

Sandy Soil Moisture Measurement

Loamy Soil Moisture Measurement
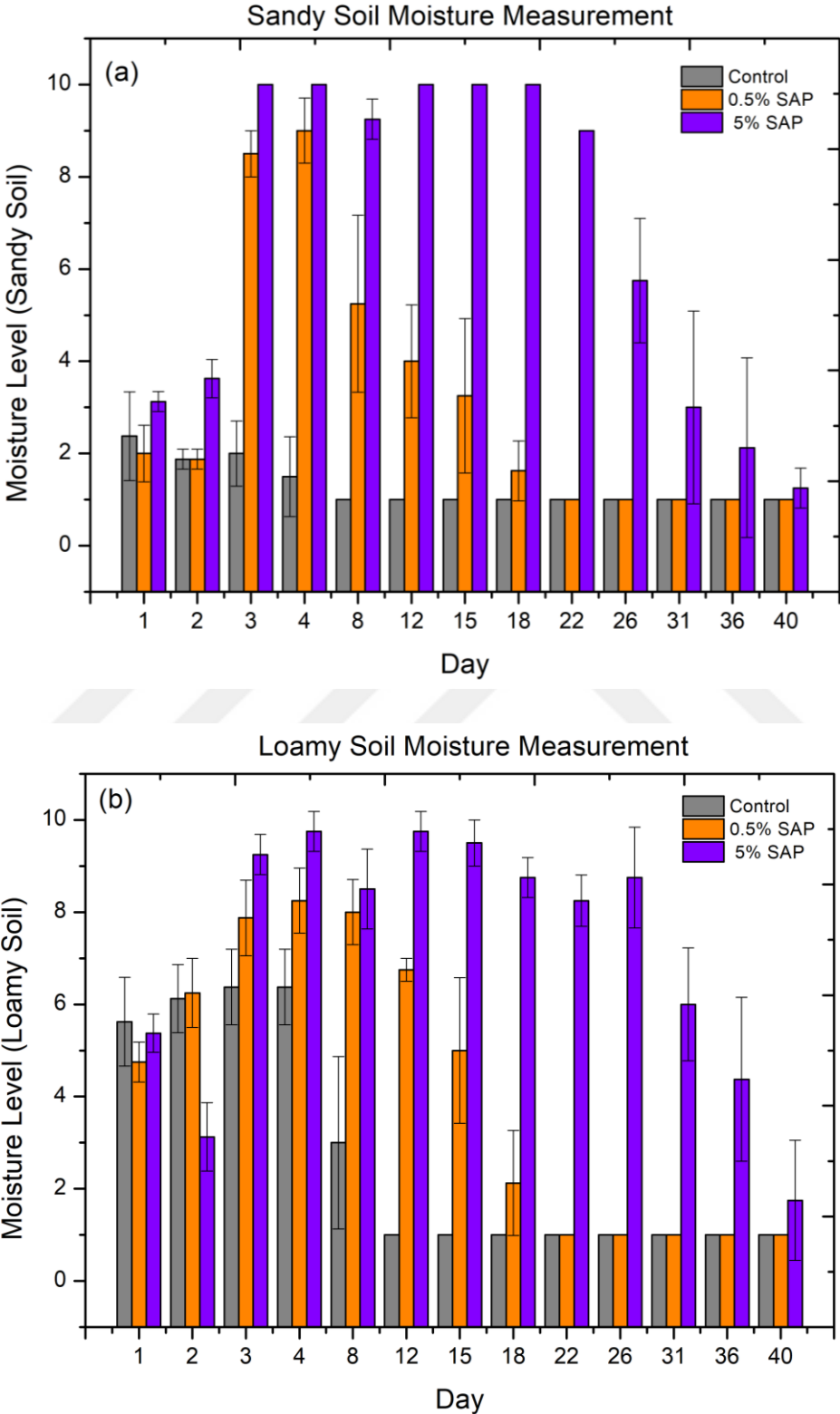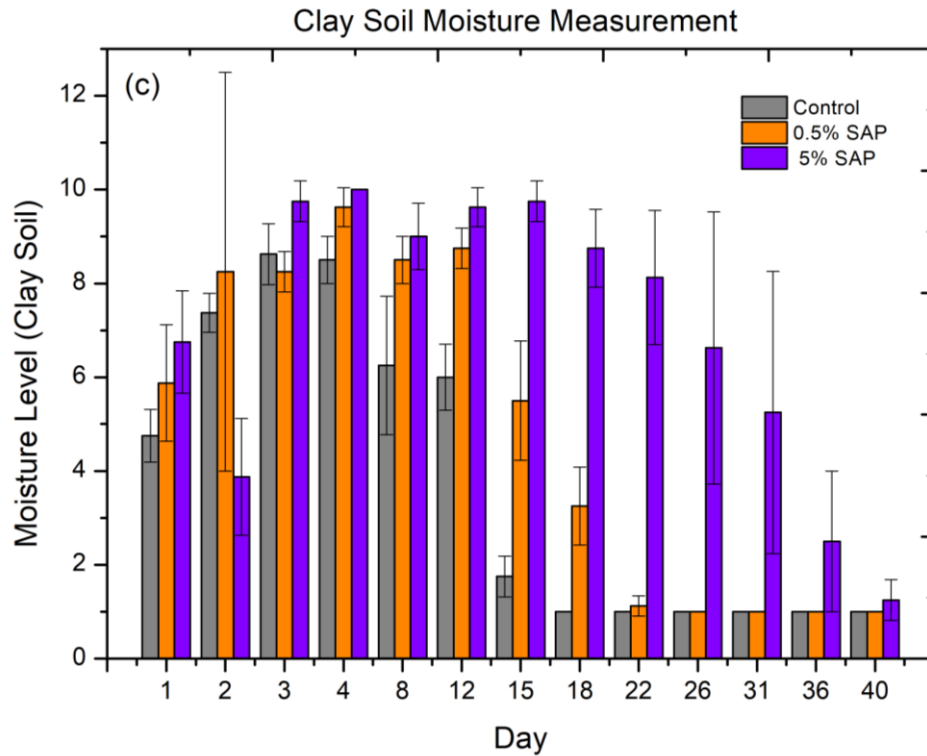
Figure 3.8 The results of soil moisture level measurement in sandy (a), loamy (b), and clay (c) soil with control, 0.5%, and 5% SAP doses

In Figures 3.8 a, b and c, the maximum moisture level was reached at doses containing 0.5% and 5% SAP in 3 different soil types on the 4th day. Then the soil moisture level decreased over time as irrigation was stopped. On the 12th day, the soil blended to mix soil and swollen SAPs. Thus the moisture level increased in the clay soil containing 0.5% SAP and in sandy, loamy, and clay soil containing 5% SAP.

On the 4th day, at the maximum soil moisture level, the moisture level increased 5 times with 0.5% SAP and 7 times with 5% SAP compared to the control group in the sandy soil, which is unsuitable for agriculture. After reaching the maximum moisture level in the sandy soil, the moisture level was preserved for 12 and 28 times longer with 0.5% and 5% SAP doses than the control group. Maximum soil moisture level in loamy soil was increased 1.3 and 1.6 times with 0.5% and 5% SAP, respectively. In addition to the increase in the maximum moisture level, it was observed that the soil moisture level was maintained 3.5 times longer with 0.5% SAP and 9 times longer with 5% SAP compared to the control group. This increase in the preservation of the maximum moisture level in the soil is the prolonged slow water release due to the presence of SAPs.

31

Although a significant increase was not observed in the maximum soil moisture level of clay soil, the moisture level was maintained for 1.5 times longer with 0.5% SAP compared to the control group. Also, with 5% SAP, the maximum soil moisture level was increased 1.5 times. On the other hand, at the end of the 40th day, it was observed that the soil moisture level was preserved the longest time in the loamy soil containing 5% SAP. Therefore, the soil moisture level was maintained 3 times longer than the control group.

3.7. Conclusions

Nanocomposite hydrogels with varying nanofiller content, high swelling capacities, and longer release times were designed and synthesized by the free radical copolymerization of AM, AA, and AMPS in water. The crosslinked hydrogels and nanocomposite hydrogels were characterized by structural, thermal, mechanical, and swelling properties. It was confirmed from FTIR results all monomers participated in the polymerization, and HNT is available in the polymer matrix. TGA measurements demonstrate an increase in thermal degradation temperatures of nanocomposites concerning nanofiller addition, while the residual mass increase is directly proportional to the amount of added HNT. The highest swelling value is observed in the SAP2HNT5 sample, which has the lowest calculated crosslink density. The rheological characterization of swollen SAPs reached the maximum storage modulus of 2815 Pa at 25 °C when 1% HNT and an additional amount of AA monomer were added into the polymer structure. In line with this, as it was found in the swelling/release performance test, the water release time was prolonged up to 27 days with the addition of 1-5% HNT. The highest water retention profile, particularly after day 10 is observed in SAP2HNT1, which also demonstrates the best storage modulus value. Based on all these results, the maximum swelling ratios of nanocomposite SAPs correlate with the crosslinked density of SAPs, while water retention capacities correlate with storage moduli. The rheology investigation suggested a 3-phase mechanism of HNT nanofiller-SAP interaction. In the first phase, nanoparticles are incorporated into the nanocomposite structure via secondary interactions. In the second phase, the additional amount of nanofiller induced grafting, resulting in a reduced amount of crosslinking. In the third phase, nanofiller agglomerates take place; and the modulus responses becomes fluctuated. A similar non-monotonous trend is observed in calculated in swelling experiments of SAP-HNT nanocomposites, but this time the trend is governed by crosslink densities rather than the HNT nanofiller.

In line with soil moisture results, it has been observed that the soil moisture level is preserved for a long time in drought regions thanks to the long-term water release of SAP-HNT

nanocomposites. In addition, unsuitable soils such as sandy soil can be made suitable for agriculture. The current study is a valuable explanation structure-function relationship for SAP-based nanocomposites and provides insights for the future designs of smart hydrogels.

Chapter 4

Chapter 4 comprises the investigation of the swelling performance of hydrogels synthesized with tunable crosslink densities. First, to see the effect of crosslinker amount on the swelling performance of hydrogels clearly, poly(ethylene glycol) diacrylate (PEGDA) monomer was synthesized to be used as a crosslinking agent. In the next step, the synthesis of SAPs was carried out with different amounts and chain lengths of PEGDA crosslinkers instead of vinyltrimethoxy silane (VTMS) crosslinker.

4. Experimental Methodology

4.1. Materials

Polyethylene glycol 4000, 2000, and 1000 (PEG4000, PEG2000 PEG1000) were purchased from Sigma Aldrich. Acryloyl chloride, 96%, stab. with phenothiazine, was purchased from Gute Chemie and used as received. Triethylamine (TEA) for synthesis and toluene were obtained from Merck Millipore and used without any further purification.

4.2. Synthesis of PEGDA Crosslinker

PEG 4000, 2000 and 1000 were used to synthesis three different crosslinkers in different chain lengths. First, to synthesis PEGDA1 crosslinker with the reaction of PEG 4000 and acryloyl chloride, PEG4000 was stirred in toluene at 120°C for 24 hours under azeotropic distillation to remove water in the reaction environment. To capture the HCl gas, which is the result of the PEG and acryloyl chloride reaction, triethylamine was added to PEG-toluene solution after the solution temperature reached to room temperature. After stirred PEG-TEA-toluene solution for 5 minutes, acryloyl chloride was dropped to mixture slowly and continued stirring solution for 24 hours at room temperature. The equivalent mole ratios of PEG molecules to acryloyl chloride were determined 1:2 to react acryloyl chloride with both hydroxyl end groups of PEG chains. The equivalent mole amounts of reactants are presented in Table 4.1. At the end of the 24 hours, the reaction was completed and PEGDA monomer was obtained as a precipitating white powder. The precipitated part was washed a few times with toluene and hexane, respectively under vacuum filtration. The filtered PEGDA monomer was dried at room temperature to remove any residual solvent. PEGDA2 and PEGDA3 monomers were synthesized with PEG 2000 and PEG 1000, respectively with the same method. The reaction mechanism of PEGDA monomer synthesis is presented in Figure 4.1.

Table 4.1 The equivalent mole amount of reactants for the PEGDA crosslinker monomer synthesis

Sample	Reactants	Equivalent Mol Amount
PEDA1	**PEG 4000**	0.01
	Acryloyl chloride	0.02
	Triethylamine	0.02
	Toluene	1.5
PEGDA2	**PEG 2000**	0.01
	Acryloyl chloride	0.02
	Triethylamine	0.02
	Toluene	1.5
PEGDA3	**PEG 1000**	0.01
	Acryloyl chloride	0.02
	Triethylamine	0.02
	Toluene	1.5

Poly(ethylene glycol)   Acryloyl chloride   Poly(ethylene glycol) diacrylate
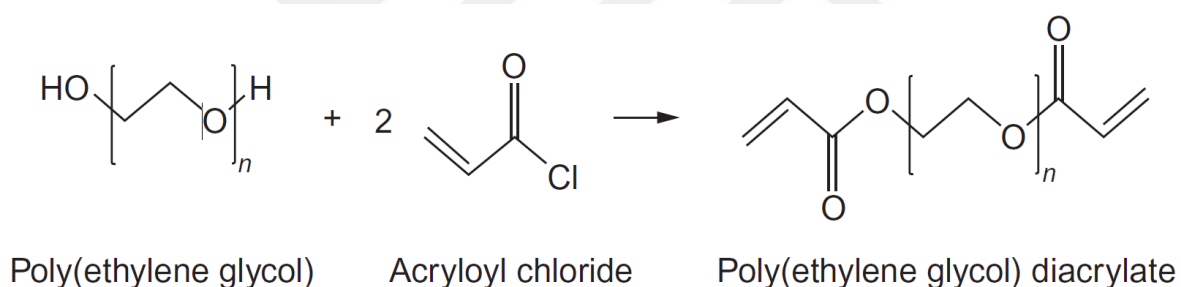
Figure 4.1 The reaction mechanism of PEGDA monomer synthesis

4.3. H NMR Characterization of Synthesized Crosslinker

1H-NMR (Nuclear Magnetic Resonance) spectra of prepared PEGDA monomers were obtained using Varian Inova Nuclear Magnetic Resonance spectrometer (500 MHz). Obtained Data was processed by MestreNova v.14 Software [73].

First, PEGDA1, PEGDA2, and PEGDA3 monomers were prepared by dissolving 2 mg of each monomer in 600 uL of deuterium water. 1H-NMR spectrums of prepared PEGDA1, PEGDA2, and PEGDA3 monomers in d-H2O are depicted in Figure 4.2-a, b, and c, respectively. The characteristic peaks corresponding to -CH units (d,e,f and g) of PEG 4000, PEG 2000 and PEG 1000 are observed around 4.35, 3.85 and 3.55 ppm. The acrylate group peaks of CH2=CH units, the result of the PEG and acryloyl chloride molecule reaction, are observed around 6.50-6.00 ppm in the PEGDA1, PEGDA2, and PEGDA3 proton NMR

spectrums. The peaks around 3.20 and 1.30 are due to the residue of excess triethylamine. Proton NMR spectrums of PEGDA1, PEGDA2, and PEGDA3 crosslinker monomers, the result of the reaction of PEG 4000, PEG 2000, and PEG 1000 separately with acryloyl chloride, confirm PEGDA monomers synthesis occurred successfully.
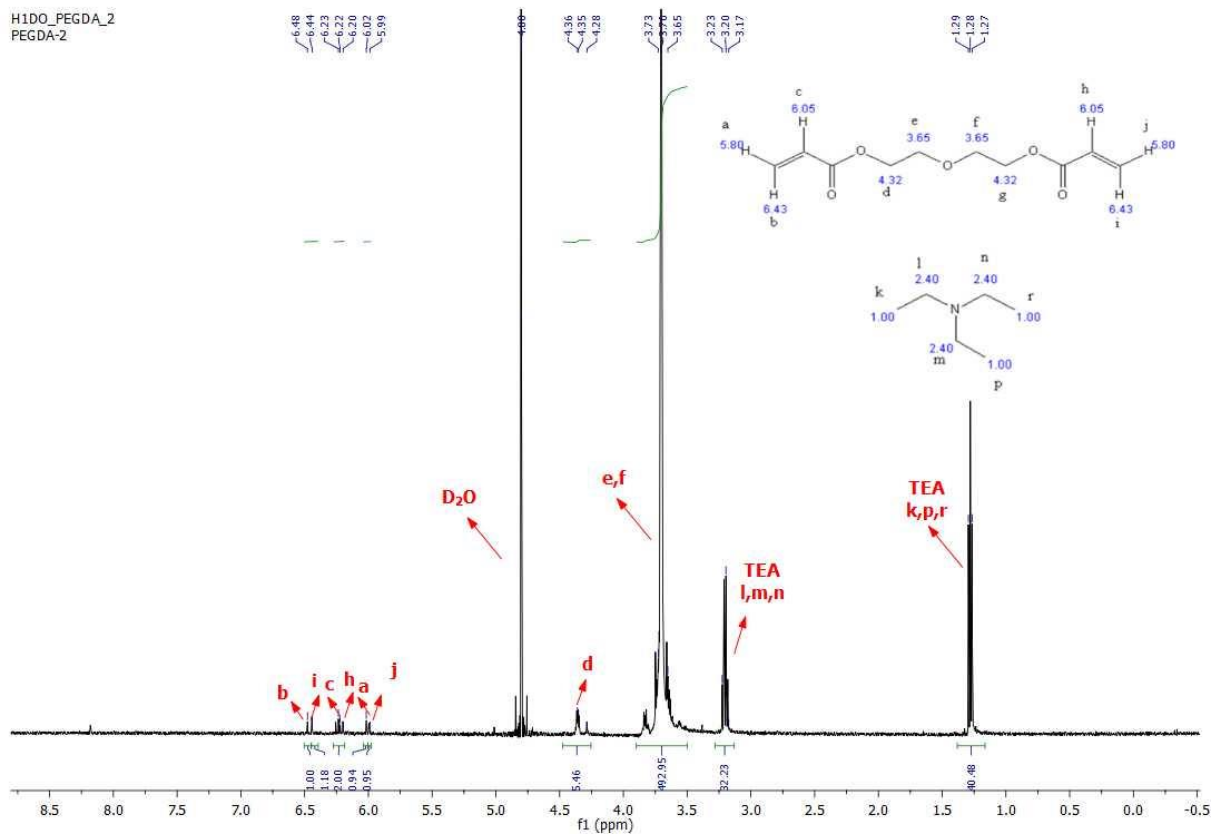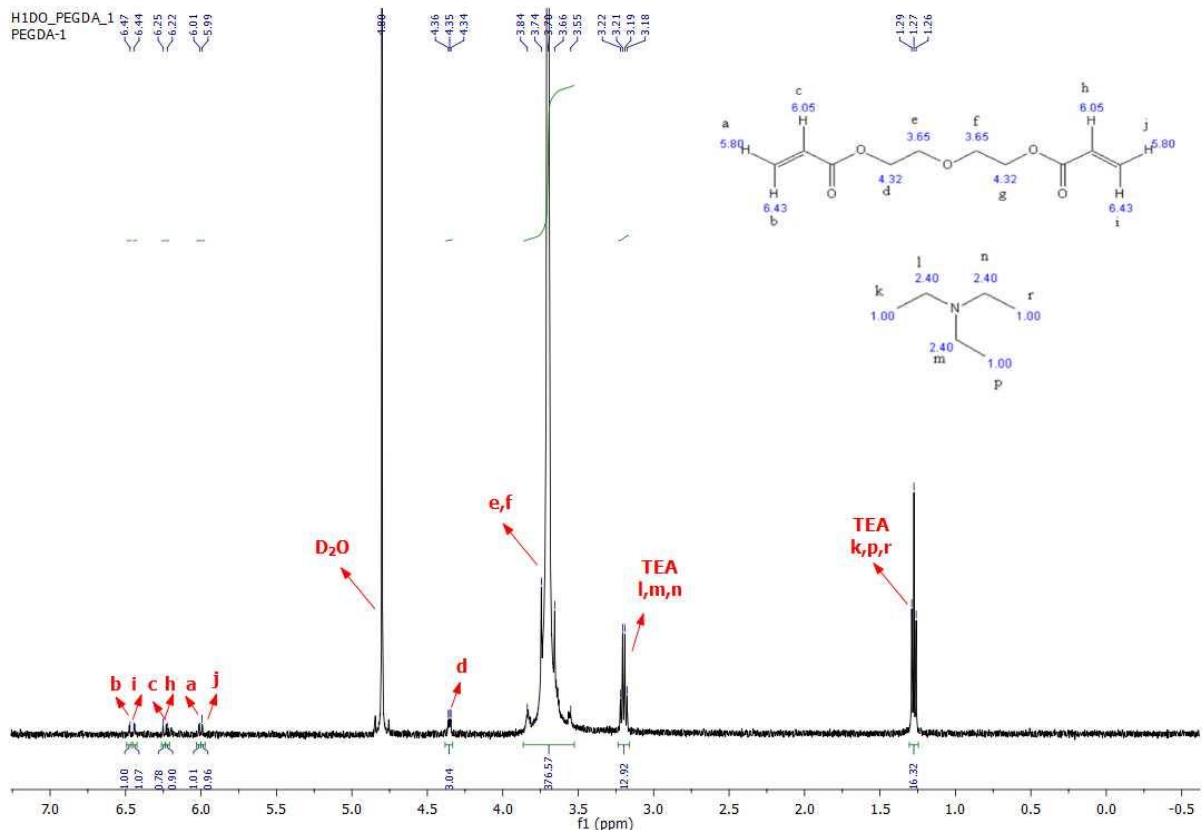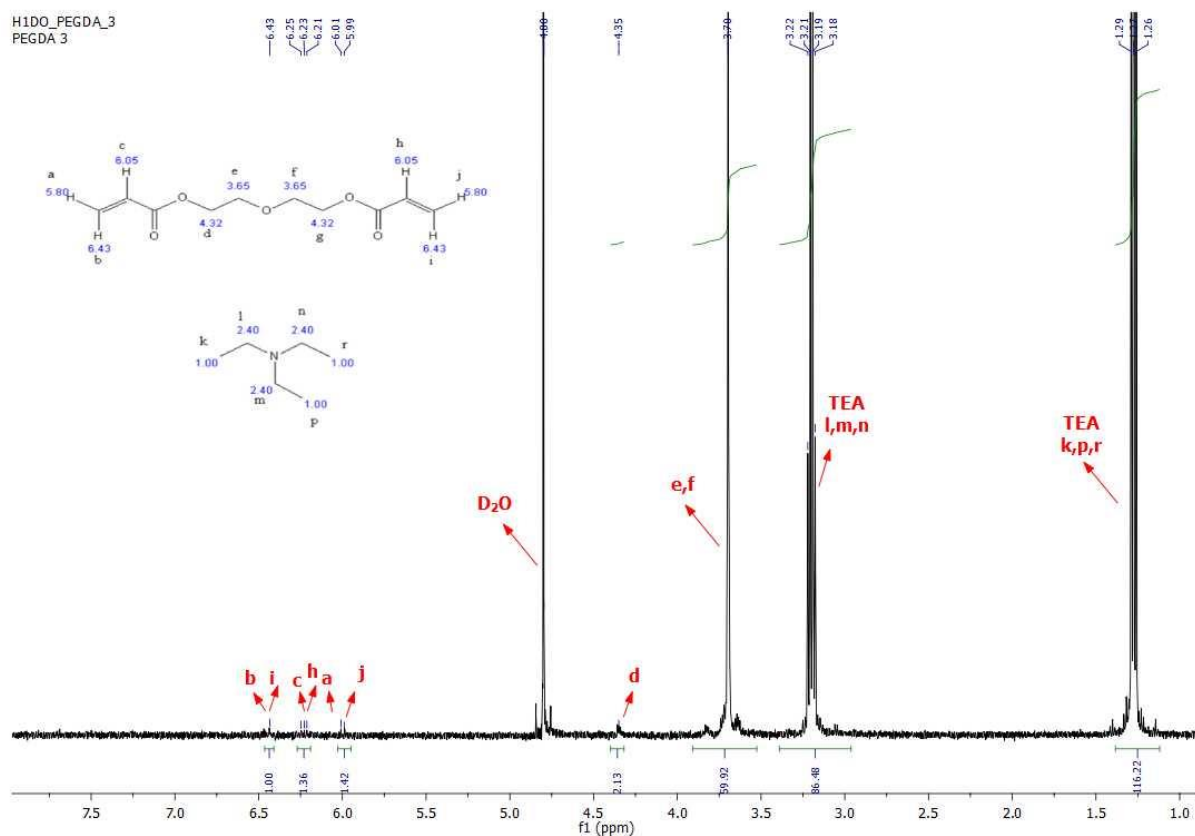
Figure 4.2 Proton NMR spectrums of PEGDA1 (a), PEGDA2 (b), and PEGDA3 (c) synthesized crosslinker monomer

4.4. Synthesis of SAPs with PEGDA Crosslinker

In the first data set, the effect of the chain length of PEG molecules on the swelling behavior of synthesized SAPs was investigated with PEGDA1, PEGDA2, and PEGDA3 crosslinkers. The tri-random copolymers were synthesized with acrylamide (AM), 2-acrylamide-2-methylpropane-1-sulphonic acid (AMPS), and acrylic acid (AA) monomers. The synthesized PEGDA monomers with three different chain lengths were used to synthesize tri-random copolymer SAPs as a crosslinker. To tune the crosslink density more precisely and prevent the occurrence of physical crosslinking due to the presence of nanotubes, HNT was not incorporated into the polymer matrix.

To observe the chain length of PEGDA crosslinker on swelling capacity, monomer, crosslinker, and initiator mole amount were kept constant. The equivalent mole ratios of monomers and crosslinker are the same as in the synthesis of SAP2HNT0 (Table 2.1). Three different SAPs, crosslinked with separate PEGDA crosslinkers, were synthesized with the same synthesis method. The determined mole amount of AM, AMPS monomers (Table 4.2) was dissolved in distilled water, then added AA monomer and PEGDA crosslinker to the

mixture. The pH of monomer mixture was adjusted to 7 with the addition of 12 M NaOH solution. The neutralized monomer solution was placed to 2-neck flask and purged with nitrogen gas for 15 min to remove oxygen in the reaction environment. Ammonium persulfate (APS) dissolved in 2 mL of distilled water was added to monomer solution and set the temperature at 70°C to initiate the reaction. At the end of the 2 hours the reaction terminated, and SAP-Px polymer are obtained in the gel form. The obtained gel was washed with ethanol to remove unreacted monomers and dried overnight at 70°C. Three different SAP-P polymers, presented in Table 4.2 were synthesized with different PEGDA crosslinkers.

Table 4.2 The equivalent mole amount of monomers and crosslinkers of SAPs synthesized with three different PEGDA crosslinkers

		SAP-P1	SAP-P2	SAP-P3
Monomers	AM	0.0600	0.0600	0.0600
	AMPS	0.0050	0.0050	0.0050
	AA	0.0700	0.0700	0.0700
Crosslinkers	PEGDA1 (PEG 4000)	0.0013	-	-
	PEGDA2 (PEG 2000)	-	0.0013	-
	PEGDA3 (PEG 1000)	-	-	0.0013
Initiator	APS	0.0003	0.0003	0.0003

The effect of crosslinker mole amount on the swelling behavior of synthesized SAPs was investigated with PEGDA1 and PEGDA2 crosslinkers in the second data set. Since the PEGDA3 crosslinker self-crosslinked with the reactive end groups over time at room temperature due to the shorter chain length, the effect of mole amount of PEGDA3 was not put on the second data set.

The amount of crosslinker was determined according to the ratio of crosslinker mol amount to the total monomer mol amount. The mol ratio of 1:100 crosslinker / total monomer was identified as the control sample, referred to as SAP-P1-2. The crosslinker mole amount was increased and decreased according to the control sample. First, the crosslinker/total monomer mole ratio was reduced to 1:85, increasing the crosslinker by 25 percent. Second, the

crosslinker amount was decreased by 25 and 75 percent, corresponding to a mole ratio of 1:150 and 1:450 crosslinker / total monomer. The determined crosslinker monomer mole amounts for PEGDA1 and PEGDA2 were presented in Table 4.3.

Table 4.3 The crosslinker mol amounts of synthesized SAP-P data sets

		SAP-P1-1	SAP-P1-2	SAP-P1-3	SAP-P1-4
Monomers	AM	0.0600	0.0600	0.0600	0.0600
	AMPS	0.0050	0.0050	0.0050	0.0050
	AA	0.0700	0.0700	0.0700	0.0700
Crosslinker	PEGDA1	0.0016	0.0013	0.0009	0.0003
Initiator	APS	0.0003	0.0003	0.0003	0.0003
		SAP-P2-1	**SAP-P2-2**	**SAP-P2-3**	**SAP-P2-4**
Monomers	AM	0.0600	0.0600	0.0600	0.0600
	AMPS	0.0050	0.0050	0.0050	0.0050
	AA	0.0700	0.0700	0.0700	0.0700
Crosslinker	PEGDA2	0.0016	0.0013	0.0009	0.0003
Initiator	APS	0.0003	0.0003	0.0003	0.0003

SAP-P1 and SAP-P2 polymers in Table 4.3 were synthesized with the same polymerization method, and the dried polymers were ground to prepare for swelling tests.

4.5. Swelling Performance Test of SAPs

The swelling performances of synthesized SAP-P set with different PEGDA crosslinkers were investigated using the SAP2 data set equilibrium swelling measurement method in Chapter 2.4. First, the equilibrium swelling ratios were calculated as in Equation 1:

$$ESR(g/g) = \frac{W_s - W_d}{Wd}$$

Where W_s is the weight of hydrogel at equilibrium and W_d is the weight of the dry polymer.

After the hydrogel reaches the maximum swelling capacity, in other words, the equilibrium swelling ratio, the gel begins to release water inside the polymer structure. The water release ratios were calculated with the same equation (Eq 1); only the ESR mark was changed to EShR to emphasize the difference between swelling and release ratios.

First, to observe the effect of crosslinker chain length on the swelling behavior of SAPs, the swelling ratios of synthesized SAP-P1, SAP-P2, and SAP-P3 polymers with three different crosslinkers were measured in distilled water. At the end of the four hours, SAP-P1, SAP-P2, and SAP-P3 all polymers were reached the maximum swelling ratio values. Furthermore, as the different crosslinkers were used and HNT was not incorporated into the polymer structure, the SAP-P data set achieved the maximum swelling ratios faster than the SAP2HNT data set in Chapter 2.

When the maximum swelling ratios are compared between the SAP-P data set samples, the maximum swelling ratio was obtained 225 g/g with SAP-P3, presented in Figure 4.3. However, SAP-P3 was synthesized with the PEGDA3 crosslinker comprised of the PEG 1000 molecule, the shortest PEG molecule in the data set. As the molecular weight of the PEG molecule increases, the swelling ratio of hydrogel increases but Figure 4.3 shows an inverse proportion between molecular weights and swelling ratios. The reason behind this result is related to the crystallization degree of SAP-Px data set polymers. It can be observed from the DSC results of SAP-Px polymers (Chapter 4.6), Table 4.4, and Fig 4.9b; the crystallization enthalpies increase with increasing PEGDA chain length. This is because the chain length of the PEGDA crosslinker rises with the higher molecular weight of PEG molecules. In this way, the segmental mobility of PEGDA molecules decreases, and the geometric alignment is more ordered. Also, the longer chain length of PEGDA crosslinkers is prepared with a higher molecular weight of PEG molecules. This might cause an increase in the chain entanglements

of crosslinkers and reduce the stability of longer chains. Therefore, the swelling abilities of SAP-Px drop away due to the critical entanglement molecular weight of PEG[74].
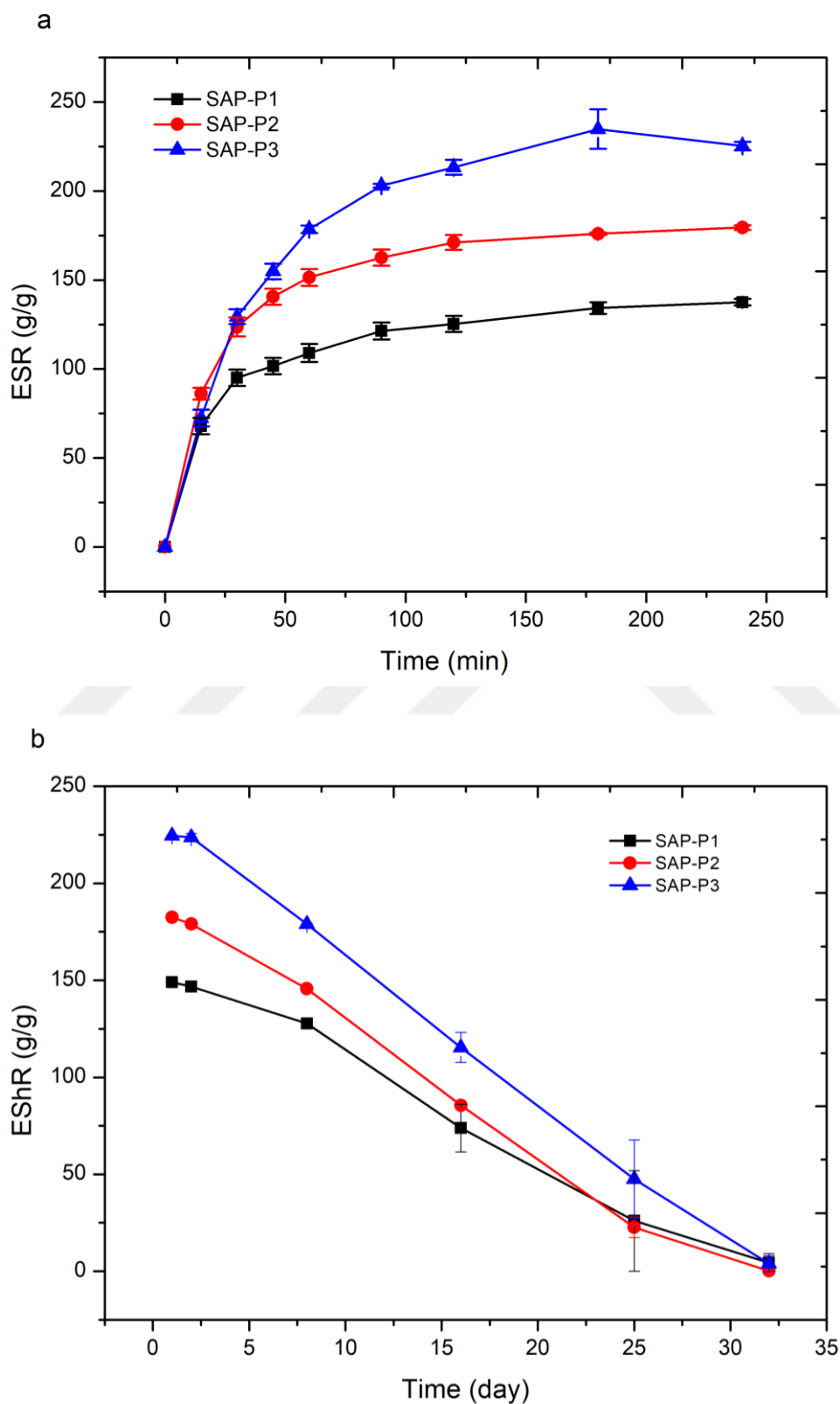
Figure 4.3 The equilibrium swelling (a) and water release (b) ratios of SAP-P data set consist of three different PEDGA crosslinkers
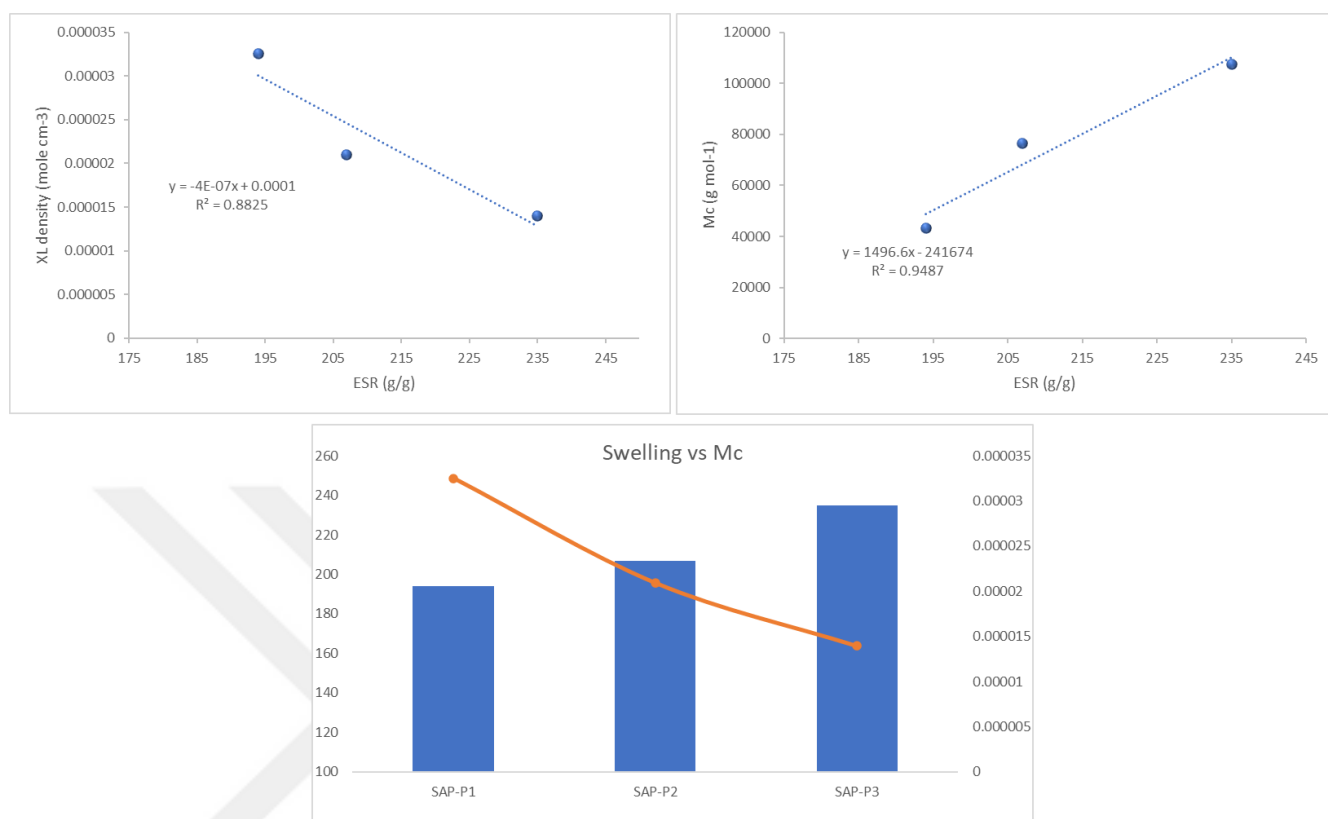
Figure 4.4 The relationship between crosslinked density (a), molecular weight between crosslinks, Mc (b), and maximum swelling ratios (c)

SAP-P1-x and SAP-P2-x data sets were prepared to describe the impact of crosslinker mol amount on swelling capacities. As the crosslinker amount decreases, the crosslink density of SAP decreases, and as a result, the swelling degrees of SAPs increase. The inverse proportion between the crosslinker amount and swelling ratios was confirmed with SAP-P1-x .and SAP-P2-x data sets (Figure 4.5 and Figure 4.6). The minimum swelling ratios were observed with SAP-P1-1 and SAP-P2-1 since they have maximum crosslink densities due to higher crosslinker amounts. Furthermore, the maximum swelling capacities were reached with SAP-P1-4 and SAP-P2-4 because of their minimum crosslinker amount.

No change was observed in the water release time of SAPs synthesized with different chain length crosslinkers (Fig 4.3-b). However, Figures 4.5-b and 4.6-b show the water release time alters with the crosslinker amount. As the crosslinker amount increase, the water release time is longer because the crosslink density of SAP increases.
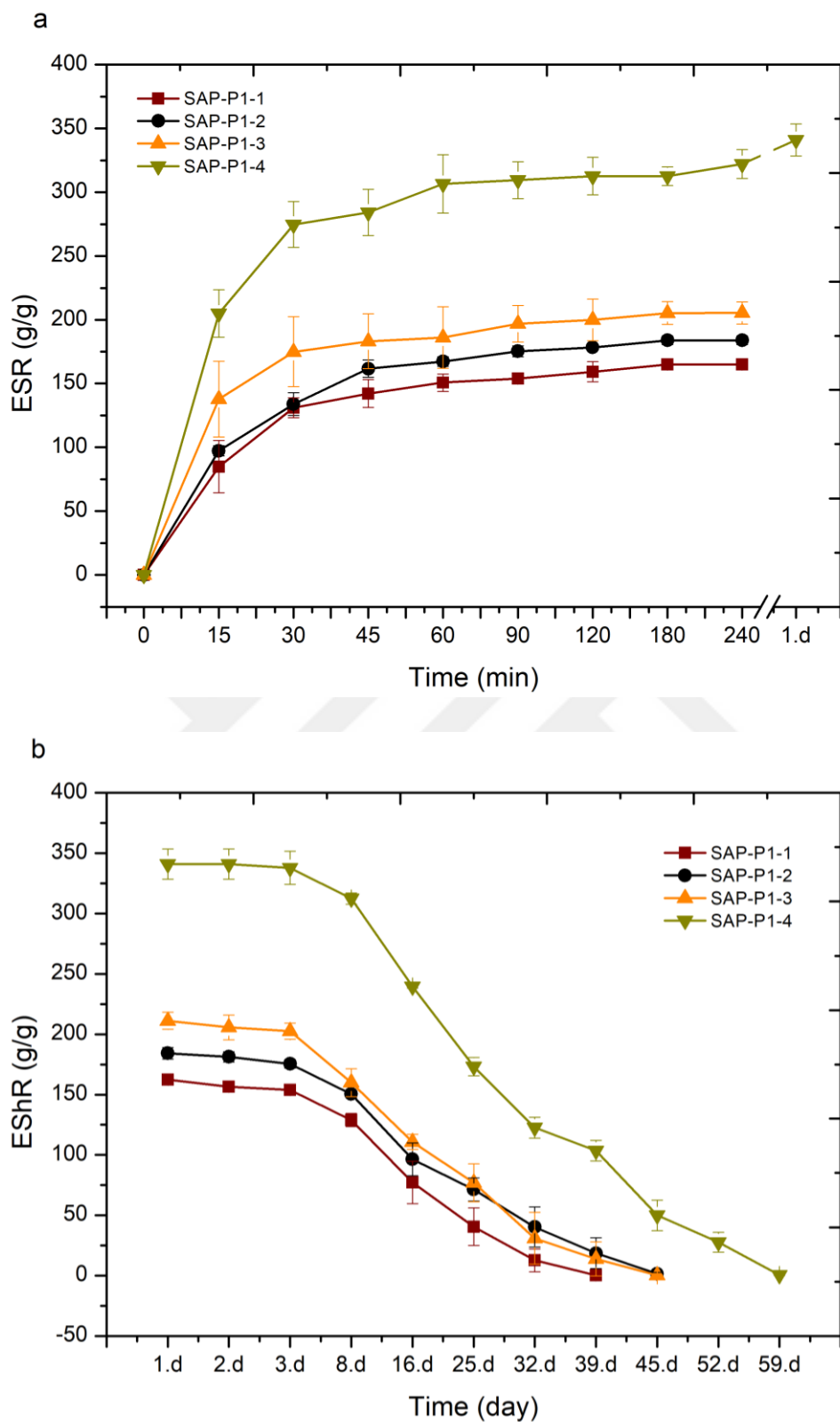
Figure 4.5 The swelling (a) and water release (b) results of SAP-P1-x data set synthesized with different crosslinker mol amounts
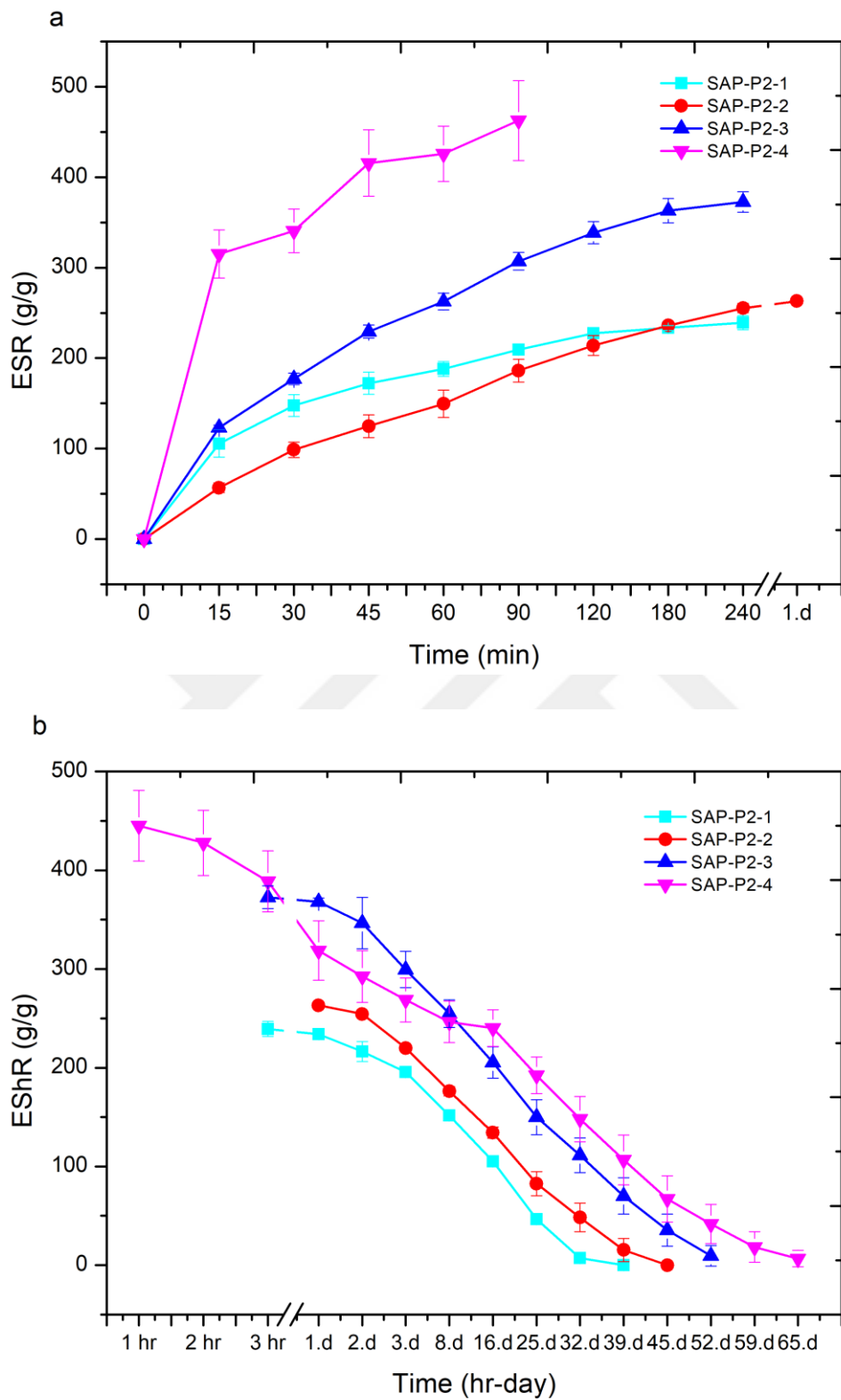
Figure 4.6 The swelling (a) and water release (b) results of SAP-P2-x data set synthesized with different crosslinker mol amounts

Figure 4.7 presents the maximum swelling values of SAP-P1-x and SAP-P2-x data sets with four different crosslinker mol amounts. In all different mol amounts, the SAP-P2-x data set reached higher swelling ratios than the SAP-P1-x data set due to the chain length difference between the crosslinkers.
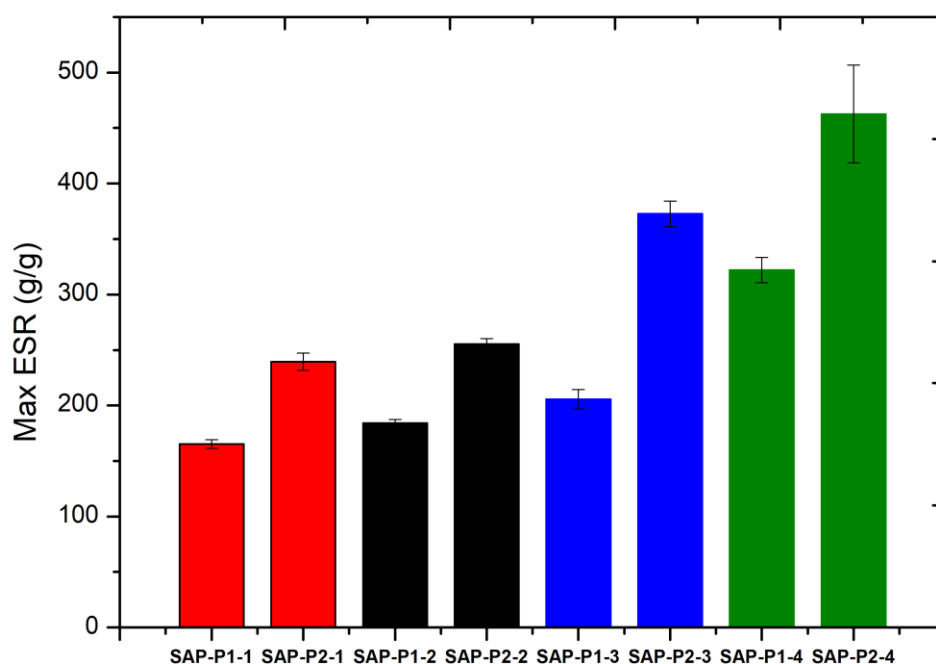
Figure 4.7 The bar chart comparison between maximum swelling ratios of SAP-P1-x and SAP-P2-x data sets

4.6.Characterizations

Thermal Characterizations

-TGA

Thermogravimetric analyses of SAP-Px data set were done by a Mettler Toledo STA (Simultaneous Thermal Analysis) differential thermogravimetric analyzer. All samples were heated from 30 to 100 °C at a linear heating rate of 10°C/min with a 50 mL/min flow under N_2 atmosphere.

Thermogravimetric analysis was conducted to determine the effect of crosslinker chain length on thermal degradation. Figure 4.3 presents the mass losses of SAP-Px data set polymers against the temperature. The mass losses of SAP-P1, SAP-P2, and SAP-3 against heating

correlate with the chain length of crosslinkers. Since SAP-P1 was synthesized with the PEGDA1 crosslinker comprising PEG4000, the most extended chain length of PEG molecule in the data set, the maximum rate of weight loss at 400°C belongs to SAP-P1 with 65% amount. SAP-P1 and SAP-P2 comprising PEG2000 and PEG1000, respectively, exhibited a similar thermal degradation trend between 250 and 450 °C due to the chain length of crosslinkers. In addition, a decrease was observed in the thermal stabilities of SAP-Px data set polymers with the extended chain length of the crosslinker. However, the thermal stability of SAP-P2 and SAP-P3 exhibited almost no difference as they comprise of the shorter chain length crosslinker as against SAP-P1.
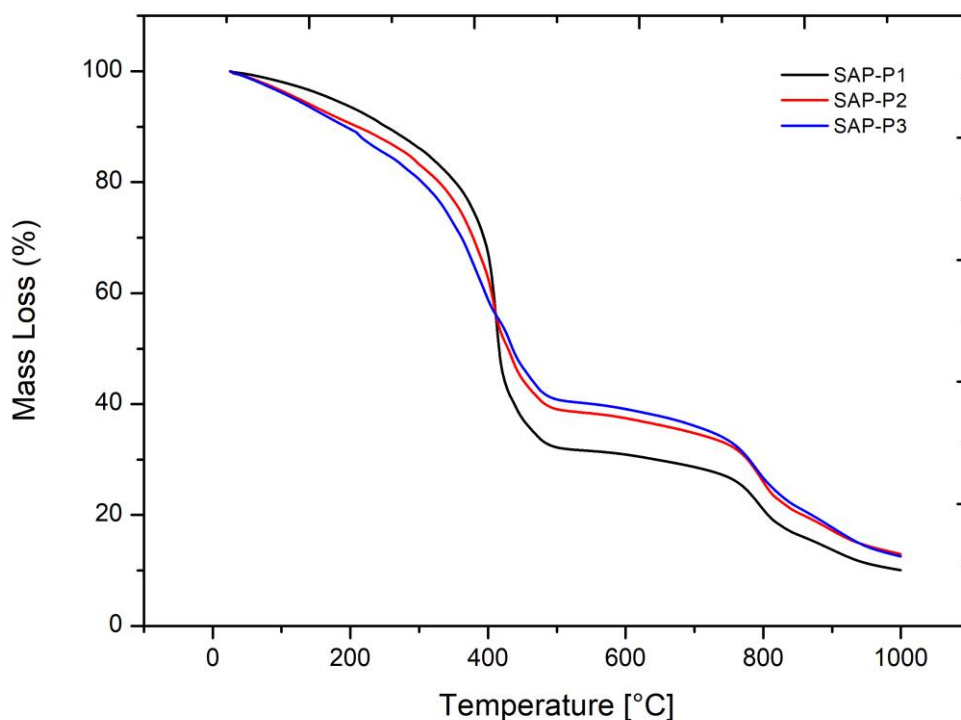
Figure 4.8 TGA curves for SAP-Px under nitrogen atmosphere

- DSC

Differential Scanning Calorimetry (DSC) analyses were performed on a TA Q2000 instrument. All measurements were examined in the range of 25 and 350°C with a 50 mL/min flow rate at a linear heating and cooling rate of 10 °C/min under N_2 atmosphere. First, the heating was started from 25 to 350° C with a heating rate of 10°C/min and cooled from 350 to

25 °C with a 10°C/min cooling rate. Then, the second heating cycle was done from 25 to 350°C again.

The simultaneous Differential Scanning Calorimetry (DSC) curves of the first heating and cooling cycles of synthesized SAP-P1, SAP-P2, and SAP-P3 are presented in Figures 4.9-a and b. Two prominent regions between 30°C -60°C and 200°C -300°C are observed in the heating curves. The small peaks at 100°C in the SAP-P2 and SAP-P3 curves are attributed to the loss of adsorbed water. The first melting peaks in the range of 30-60°C correspond to the melting of PEGDA crosslinkers. Therefore, the melting-peak enthalpy values presented in Table 4.4 are directly proportional to the chain length of PEGDA crosslinkers. As the crosslinker chain length increase, the enthalpy of melting-peak increases. This is because more energy is released when the crosslinkers with longer chain lengths melt.

SAP-Px data set polymers are composed of AA-AM-AMPS random triblock copolymers, crosslinked with PEGDA crosslinkers in three different chain lengths. The peaks around the 200°C -300°C are related to the functional groups of monomers in the polymer backbone. The endothermic peaks around 210-230°C correspond to the degradation of amide groups of AM and AMPS. The sulphonic groups of AMPS begin to degrade around 250°C, and these flow by the polymer backbone degradation.

48
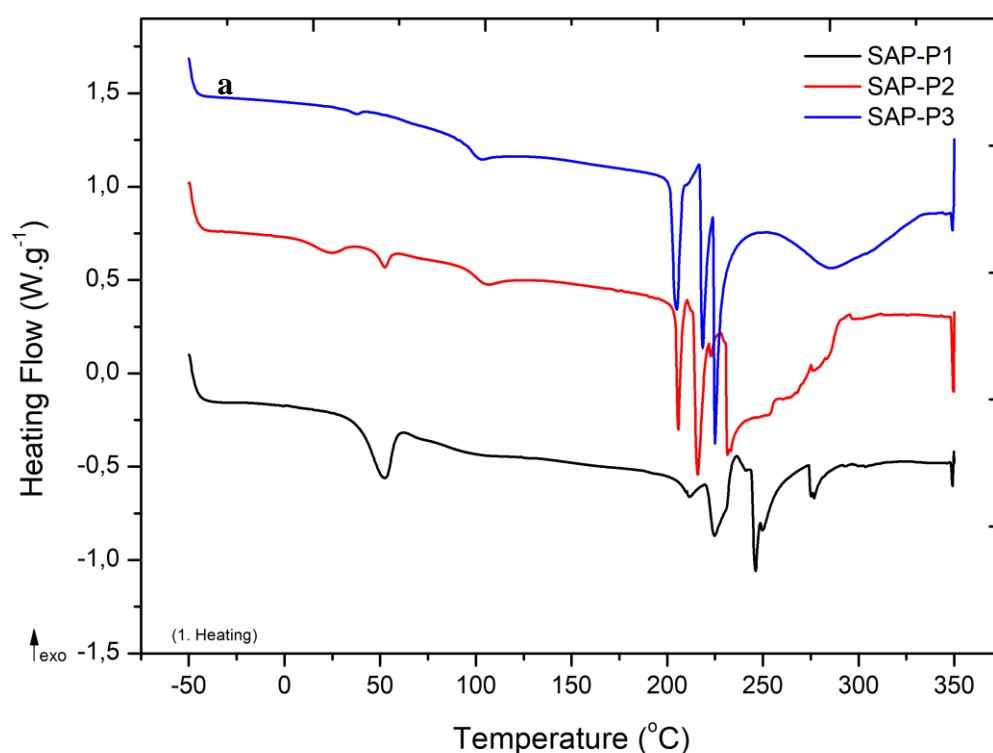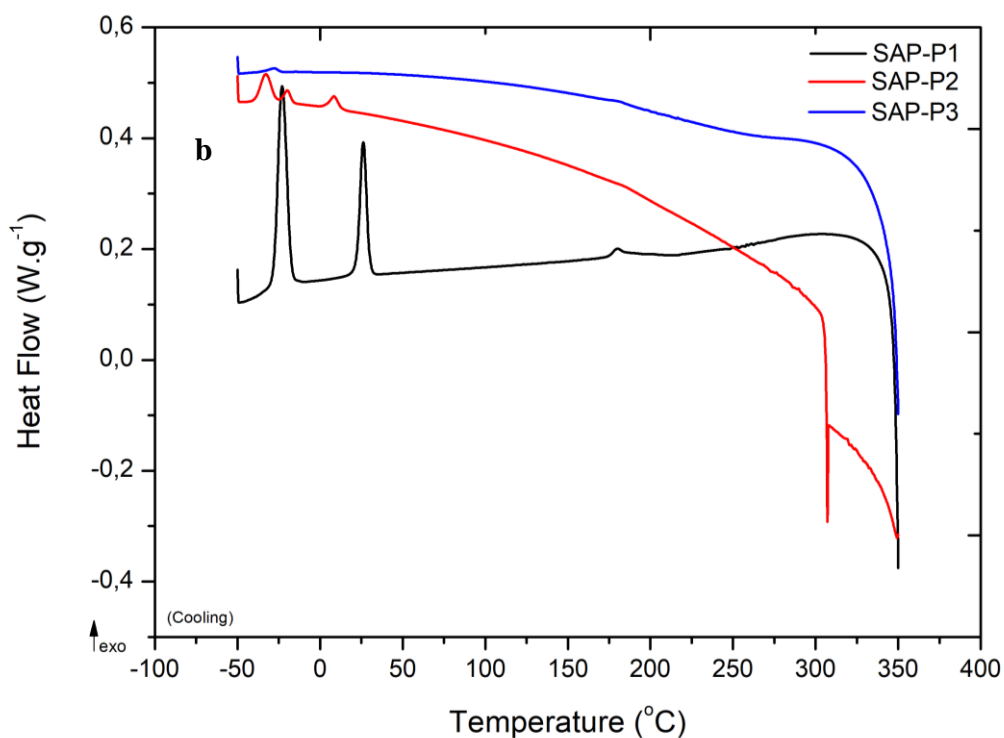
Figure 4.9 First heating (a) and cooling (b) DSC curves for SAP-Px data set under nitrogen atmosphere

The cooling cycles of SAP-P1, SAP-P2, and SAP-P3 are presented in Figure 4.9-b. Two exothermic crystalization peaks in the range of -40°C -20°C are related to the crystallization of PEGDA crosslinkers. The enthalpies of crystallization peaks are directly proportional with the chain lengths of crosslinkers, similar to the melting peaks in Figure 4.9-a.

Enthalpies ⟶ Samples ↓	Tm (°C)	Tc (°C)	ΔH_m (J/g)	ΔH_c (J/g)
SAP-P1	52	-23 and 26	20.01	21.86
SAP-P2	24 and 53	-27 and 13	7.51	4.15
SAP-P3	37	-	0.47	0

Table 4.4 DSC Heating and cooling curves results of SAP-Px data set polymers

Furthermore, a relationship is observed between crystallization degree and equilibrium swelling ratios of SAP-Px data set polymers. In Chapter 4.5, the swelling performance test results of SAP-P1, SAP-P2, and SAP-P3 give an inverse proportion between maximum swelling ratios and crosslinker chain lengths. However, as the crosslinker chain length increase, the maximum swelling ratios of SAPs should be higher. The reason behind the inverse proportion between swelling ratios and chain lengths of SAP-P1, SAP-P2, and SAP-P3 stems from their crystallization degree. Although SAP-P1 crosslinked with the most extended chain length PEGDA crosslinker (PEGDA1), it also has the highest crystallization degree. Therefore, the maximum swelling ratio of SAP-P1 is the least compared to SAP-P2 and SAP-P3. Similarly, since there was almost any crystallization peak observed in the cooling cycle of SAP-P3, the maximum swelling ratio was reached with SAP-P3.

4.7. Conclusions

This chapter has focused on the effect of chain length and mol amount of PEGDA crosslinker on the swelling capacities. First, the crosslinker chain length effect was observed with three different chain lengths of PEG molecules. PEGDA1, PEGDA2, and PEGDA3 crosslinkers were synthesized with PEG4000, PEG2000, and PEG1000, respectively. After the synthesis of PEGDA crosslinkers was confirmed by NMR characterization, the SAP-Px data set was prepared to see the crosslinker chain length effect on swelling capacities. The synthesized SAP-P1, SAP-P2, and SAP-P3 polymers are consist of the same amount of crosslinker; only the chain length of crosslinkers was changed. The obtained results from the swelling performance tests have given an inverse relation between the chain length of the crosslinker and maximum swelling ratios. The SAP-P3, synthesized with the shortest chain length crosslinker, reached the highest swelling ratio of 225 g/g compared to SAP-P1 and SAP-P3. The reason behind this is related to the crystallization degree of SAP-Px and the critical chain entanglement of the PEG molecule. The maximum swelling ratios were decreased as the crystallinity degree of SAP-Px increased. This inverse relation was also supported by the TGA and DSC thermal results. The highest crystallization degree was observed in the DSC curves of SAP-P1, synthesized with the most extended chain of PEGDA crosslinker. Also, since the critical chain entanglement increases in the long chain of PEG, the segmental mobility of the PEGDA crosslinker decreases, and thus the swelling ability of SAP-Px reduces. After observing the effect of chain length of crosslinker, the impact of crosslinker amount was investigated. The equilibrium swelling performance test results of SAP-P1-x and SAP-P2-x data sets give an inverse proportion between crosslinker mol amount and maximum

swelling ratios. Generally, as the crosslinker mol amount increase, the crosslink density of SAPs increases. Therefore, the maximum swelling ratios reduce with the increase of crosslinker mol amount due to the limitation of the swelling ability in higher crosslink densities. The correlation between crosslinker amount and the maximum swelling ratio was confirmed in Figure 4.7. The highest swelling ratio was reached with the SAP-P2-4, comprising the shorter chain length and the least mol amount of PEGDA2 crosslinker.

Chapter 5

5. Conclusions

This thesis aims to explain the relationship between mechanical properties and water retention capacity and the correlation between swelling ratios and crosslinking density. Therefore SAP nanocomposites with enhanced water retention capacities and SAPs with tunable crosslinking densities were synthesized, respectively. The synthesized SAP nanocomposites were structurally, thermally, and rheologically characterized with FTIR, TGA, and rheometer, respectively. Also, the crosslinking densities of SAP nanocomposites were calculated and compared with swelling performance tests to observe the correlation between crosslink density and swelling capacities. The incorporation of HNT nanoparticles into the polymer matrix was confirmed via FTIR, TGA, and rheology results. The synthesized triblock random AA-AM-AMPS polymers are prepared with different amounts of HNT. The TGA results of SAP-HNT nanocomposites prove the incorporation of HNT into polymer structure with the correlation between residue masses and HNT amount. The maximum swelling ratio was reached with SAP2HNT5, with minimum crosslink density. The water retention capacities were observed via a release performance test. These test results correlate equilibrium release ratios (EShR) and storage modulus and rheology results. While the water retention capacity was prolonged up to 28 days with 1% HNT addition (SAP2HNT1), and maximum storage modulus of 2815 Pa was also obtained with the rheological characterization of swollen SAP2HNT1. Based on all these results, while water retention capacities correlate with storage moduli, the maximum swelling ratios of nanocomposite SAPs correlate with the crosslinked density of SAPs. SAP-HNT nanofiller interaction was explained with a 3-phase mechanism according to rheology results. In the first phase, secondary interactions generate between nanoparticles and polymer structure. In the second phase, crosslinking reduces due to the graft polymerization with the additional amount of HNT. Finally, the modulus results fluctuate in the third phase because the HNT nanofiller aggregations form in the nanocomposite structures.

For future studies, preliminary test results of synthesized SAPs with three different PEGDA crosslinkers indicate that a detailed swelling performance test should be done at different temperatures to investigate the effect of crystallinity degree and critical chain entanglement on swelling ratios. Furthermore, the addition of HNT nanofiller into the polymer matrix may be repeated with SAP-P data set polymers to observe the PEGDA crosslinker effect on the HNT-SAP interaction mechanisms. According to the first results of SAPs synthesized with

PEGDA crosslinker, a tunable crosslink density mechanism can be provided by controlling the type and amount of crosslinkers. In this way, SAP synthesis with the desired properties is possible according to the application area.

In light of these results, the current study is a valuable explanation structure-function relationship for SAP-based nanocomposites and provides insights for the future designs of smart hydrogels.

References

1. Ma, X. and G. Wen, *Development history and synthesis of super-absorbent polymers: a review.* Journal of Polymer Research, 2020. **27**(6): p. 1-12.

2. Buchholz, F.L., *Superabsorbent polymers: an idea whose time has come.* Journal of chemical education, 1996. **73**(6): p. 512.

3. Harper, B.G., R.N. Bashaw, and B.L. Atkins, *Absorbent product containing a hydrocelloidal composition.* 1972, Google Patents.

4. El-Rehim, H.A., E.S.A. Hegazy, and H.A. El-Mohdy, *Radiation synthesis of hydrogels to enhance sandy soils water retention and increase plant performance.* Journal of applied polymer science, 2004. **93**(3): p. 1360-1371.

5. Zohuriaan-Mehr, M., et al., *Advances in non-hygienic applications of superabsorbent hydrogel materials.* Journal of materials science, 2010. **45**(21): p. 5711-5735.

6. Batista, R.A., et al., *Hydrogel as an alternative structure for food packaging systems.* Carbohydrate polymers, 2019. **205**: p. 106-116.

7. Bhuiyan, M., et al., *Improvement of swelling behaviour of poly (vinyl pyrrolidone) and acrylic acid blend hydrogel prepared by the application of gamma radiation.* Org Chem Curr Res, 2015. **4**: p. 138-145.

8. Wang, Y., et al., *Stretchable, conductive, and self-healing hydrogel with super metal adhesion.* Chemistry of Materials, 2018. **30**(13): p. 4289-4297.

9. Yang, F., et al., *A template-hatched method towards poly (acrylic acid) hydrogel spheres with ultrahigh ion exchange capacity and robust adsorption of environmental toxins.* Journal of industrial and engineering chemistry, 2019. **69**: p. 422-431.

10. Atta, A.M., A.A. Gaser, and Z.F. Kamel, *Swelling Behavior of pH-Sensitive Copolymers Containing 2-Acrylamido-2-Methyl Propane Sulfonic Acid and Acrylic Acid Crosslinked with Vinyl Trimethoxy Silane Crosslinker.* Journal of dispersion science and technology, 2010. **31**(11): p. 1456-1464.

11. Scott, A.J., T.A. Duever, and A. Penlidis, *The role of pH, ionic strength and monomer concentration on the terpolymerization of 2-acrylamido-2-methylpropane sulfonic acid, acrylamide and acrylic acid.* Polymer, 2019. **177**: p. 214-230.

12. Kabiri, K., et al., *Superabsorbent hydrogel composites and nanocomposites: a review.* Polymer Composites, 2011. **32**(2): p. 277-289.

13. Behera, S. and P.A. Mahanwar, *Superabsorbent polymers in agriculture and other applications: a review.* Polymer-Plastics Technology and Materials, 2020. **59**(4): p. 341-356.

14. Kabir, S.F., et al., *Cellulose-based hydrogel materials: chemistry, properties and their prospective applications.* Progress in biomaterials, 2018. **7**(3): p. 153-174.

15. Sadeghi, M. and F. Soleimani, *Synthesis of pH-sensitive hydrogel based on starch-polyacrylate superabsorbent.* 2012.

16. Dinescu, S., et al., *Collagen-Based Hydrogels and Their Applications for Tissue Engineering and Regenerative Medicine.* 2018.

17. Zhang, X. and G. Yang, *Application of Sodium Alginate Hydrogel.*

18. Song, S., et al., *Carboxymethyl Chitosan Modified Carbon Nanoparticle for Controlled Emamectin Benzoate Delivery: Improved Solubility, pH-Responsive Release, and Sustainable Pest Control.* ACS applied materials & interfaces, 2019. **11**(37): p. 34258-34267.

19. Tang, Y., et al., *Preparation and absorption studies of poly (acrylic acid-co-2-acrylamide-2-methyl-1-propane sulfonic acid)/graphene oxide superabsorbent composite.* Polymer Bulletin, 2019. **76**(3): p. 1383-1399.

20. Wu, F., et al., *Synthesis and characterization of a novel cellulose-g-poly (acrylic acid-co-acrylamide) superabsorbent composite based on flax yarn waste.* Carbohydrate Polymers, 2012. **87**(4): p. 2519-2525.

21.   Kiatkamjornwong, S. and P. Phunchareon, *Influence of reaction parameters on water absorption of neutralized poly (acrylic acid-co-acrylamide) synthesized by inverse suspension polymerization.* Journal of applied polymer science, 1999. **72**(10): p. 1349-1366.

22.   Bajpai, S., M. Bajpai, and L. Sharma, *Inverse suspension polymerization of poly (methacrylic acid-co-partially neutralized acrylic acid) superabsorbent hydrogels: synthesis and water uptake behavior.* Designed monomers and polymers, 2007. **10**(2): p. 181-192.

23.   Chauhan, G.S., et al., *Synthesis and characterization of acrylamide and 2-hydroxyethyl methacrylate hydrogels for use in metal ion uptake studies.* Desalination, 2009. **243**(1-3): p. 95-108.

24.   Patachia, S. and C. Croitoru, *Increasing the adsorption capacity and selectivity of poly (vinyl alcohol) hydrogels by an alternative imprinting technique.* Journal of Applied Polymer Science, 2015. **132**(23).

25.   Benda, D., J. Šňupárek, and V. Čermák, *Inverse suspension polymerization of the hydrophilic acrylic monomers in the static continuous phase.* Journal of dispersion science and technology, 1997. **18**(2): p. 115-121.

26.   Ahmed, E.M., *Hydrogel: Preparation, characterization, and applications: A review.* Journal of advanced research, 2015. **6**(2): p. 105-121.

27.   Singh, A., et al., *Hydrogels: a review.* Int J Pharm Sci Rev Res, 2010. **4**(2): p. 97-105.

28.   Bao, Y., J. Ma, and N. Li, *Synthesis and swelling behaviors of sodium carboxymethyl cellulose-g-poly (AA-co-AM-co-AMPS)/MMT superabsorbent hydrogel.* Carbohydrate Polymers, 2011. **84**(1): p. 76-82.

29.   Chaudhuri, S.D., et al., *Tuning the swelling and rheological attributes of bentonite clay modified starch grafted polyacrylic acid based hydrogel.* Applied Clay Science, 2020. **185**: p. 105405.

30.   Chen, Q., et al., *Fundamentals of double network hydrogels.* Journal of Materials Chemistry B, 2015. **3**(18): p. 3654-3676.

31.   Chen, Q., et al., *Improvement of mechanical strength and fatigue resistance of double network hydrogels by ionic coordination interactions.* Chemistry of Materials, 2016. **28**(16): p. 5710-5720.

32.   Huang, T., et al., *A novel hydrogel with high mechanical strength: a macromolecular microsphere composite hydrogel.* Advanced Materials, 2007. **19**(12): p. 1622-1626.

33.   Gooch, J., *Super absorbent fibers.* Encyclopedic Dictionary of Polymers. Springer, New York, 2011: p. 712-714.

34.   Yu, C., K. Malakpoor, and J.M. Huyghe, *A three-dimensional transient mixed hybrid finite element model for superabsorbent polymers with strain-dependent permeability.* Soft matter, 2018. **14**(19): p. 3834-3848.

35.   Ullah, F., et al., *Classification, processing and application of hydrogels: A review.* Materials Science and Engineering: C, 2015. **57**: p. 414-433.

36.   Lin, Y., et al., *Self-healing zwitterionic sulfobetaine nanocomposite hydrogels with good mechanical properties.* RSC advances, 2019. **9**(55): p. 31806-31811.

37.   Zhang, Z., et al., *Effect of salt on phosphorylcholine-based zwitterionic polymer brushes.* Langmuir, 2016. **32**(20): p. 5048-5057.

38.   Ramachandran, R., D. Jung, and A.M. Spokoyny, *Cross-linking dots on metal oxides.* NPG Asia Materials, 2019. **11**(1): p. 1-4.

39.   Hennink, W.E. and C.F. van Nostrum, *Novel crosslinking methods to design hydrogels.* Advanced drug delivery reviews, 2012. **64**: p. 223-236.

40.   Zainal, S.H., et al., *Preparation of cellulose-based hydrogel: A review.* Journal of Materials Research and Technology, 2020.

41.   Rizwan, M., et al., *Materials diversity of Hydrogel: Synthesis, polymerization process and soil conditioning properties in agricultural field.* Journal of Advanced Research, 2021.

42.   Zhang, X., et al., *Innovative application of PVA hydrogel for the forming of porous Si3N4 ceramics via freeze-thaw technique.* Ceramics International, 2018. **44**(11): p. 13409-13413.

43.   Hu, W., et al., *Advances in crosslinking strategies of biomedical hydrogels.* Biomaterials science, 2019. **7**(3): p. 843-855.

44.   Aydın, K., *Self-crosslinkable superabsorbent hydrogels based on vinlalkoxysilanes as crosslinker.* 2013.

45.   Mattson, B., et al., *Silane-modified polymers as interphases in glass-fibre-reinforced composites: 1. Synthesis and characterisation of alkoxy-silane functionalized polymers.* Composite Interfaces, 1996. **4**(2): p. 57-76.

46.   Mattson, B., et al., *Silane-modified polymers as interphases in glass-fibre-reinforced composites: 2. Grafting and crosslinking of interphase materials.* Composite Interfaces, 1996. **4**(2): p. 77-94.

47.   Albers, P.T., et al., *Water swelling behavior of poly (ethylene glycol)-based polyurethane networks.* Macromolecules, 2020. **53**(3): p. 862-874.

48.   Schweitzer, J., et al., *Determination of the Crosslinking Density of a Silicone Elastomer.* Journal of Chemical Education, 2019. **96**(7): p. 1472-1478.

49.   Curcio, M. and N. Picci, *Polymer in agriculture: a review.* Am J Agric Biol Sci, 2008. **3**(1): p. 299-314.

50.   Bakass, M., A. Mokhlisse, and M. Lallemant, *Absorption and desorption of liquid water by a superabsorbent polymer: Effect of polymer in the drying of the soil and the quality of certain plants.* Journal of Applied Polymer Science, 2002. **83**(2): p. 234-243.

51.   Bayrac, H.N. and E. Doğan, *Impacts of climate change on agriculture sector in Turkey.* 2016.

52.   Hochmuth, H., N. Thevs, and P. He, *Water allocation and water consumption of irrigation agriculture and natural vegetation in the Heihe River watershed, NW China.* Environmental earth sciences, 2015. **73**(9): p. 5269-5279.

53.   ZOHOURIAN, M.M. and K. Kabiri, *Superabsorbent polymer materials: a review.* 2008.

54.   Al-Jabari, M., R.A. Ghyadah, and R. Alokely, *Recovery of hydrogel from baby diaper wastes and its application for enhancing soil irrigation management.* Journal of environmental management, 2019. **239**: p. 255-261.

55.   Akhter, J., et al., *Effects of hydrogel amendment on water storage of sandy loam and loam soils and seedling growth of barley, wheat and chickpea.* Plant Soil and Environment, 2004. **50**(10): p. 463-469.

56.   Neethu, T., P. Dubey, and A. Kaswala, *Prospects and Applications of Hydrogel Technology in Agriculture.* Int. J. Curr. Microbiol. App. Sci, 2018. **7**(5): p. 3155-3162.

57.   Asamatdinov, A., *New Water-Keeping Soil Additives.* Mod Chem Appl, 2018. **6**(246): p. 2.

58.   Raafat, A.I., M. Eid, and M.B. El-Arnaouty, *Radiation synthesis of superabsorbent CMC based hydrogels for agriculture applications.* Nuclear Instruments and Methods in Physics Research Section B: Beam Interactions with Materials and Atoms, 2012. **283**: p. 71-76.

59.   Zhao, C., et al., *Salt-Tolerant Superabsorbent Polymer with High Capacity of Water-Nutrient Retention Derived from Sulfamic Acid-Modified Starch.* ACS omega, 2019. **4**(3): p. 5923-5930.

60.   Guo, M., et al., *Preparation and properties of a slow-release membrane-encapsulated urea fertilizer with superabsorbent and moisture preservation.* Industrial & engineering chemistry research, 2005. **44**(12): p. 4206-4211.

61.   Finosh, G., et al., *Hybrid alginate-polyester bimodal network hydrogel for tissue engineering–Influence of structured water on long-term cellular growth.* Colloids and Surfaces B: Biointerfaces, 2015. **135**: p. 855-864.

62.   Gilarska, A., et al., *Collagen/chitosan/hyaluronic acid–based injectable hydrogels for tissue engineering applications–design, physicochemical and biological characterization.* Colloids and Surfaces B: Biointerfaces, 2018. **170**: p. 152-162.

63.   Doostmohammadi, M., et al., *Hydrogels for peptide hormones delivery: therapeutic and tissue engineering applications.* Drug design, development and therapy, 2019. **13**: p. 3405.

64.   Neufeld, L. and H. Bianco-Peled, *Pectin–chitosan physical hydrogels as potential drug delivery vehicles.* International journal of biological macromolecules, 2017. **101**: p. 852-861.

65. Zhang, J.T., et al., *Preparation of temperature-sensitive poly (N-isopropylacrylamide)/β-cyclodextrin-grafted polyethylenimine hydrogels for drug delivery.* Journal of applied polymer science, 2008. **108**(5): p. 3031-3037.

66. Flory, P.J., *Statistical mechanics of swelling of network structures.* The Journal of Chemical Physics, 1950. **18**(1): p. 108-111.

67. Khalaf, A., et al., *High performance oil resistant rubber.* 2012.

68. Goudarzi, N., M.A. Chamjangali, and A. Amin, *Calculation of Hildebrand solubility parameters of some polymers using QSPR methods based on LS-SVM technique and theoretical molecular descriptors.* Chinese Journal of Polymer Science, 2014. **32**(5): p. 587-594.

69. Giron, N.H. and M.C. Celina, *High temperature polymer degradation: Rapid IR flow-through method for volatile quantification.* Polymer Degradation and Stability, 2017. **145**: p. 93-101.

70. Rahmat, M., et al., *Silane crosslinking of poly (lactic acid): The effect of simultaneous hydrolytic degradation.* Express Polymer Letters, 2015. **9**(12).

71. Rastin, H., et al., *Transparent nanocomposite coatings based on epoxy and layered double hydroxide: Nonisothermal cure kinetics and viscoelastic behavior assessments.* Progress in Organic Coatings, 2017. **113**: p. 126-135.

72. Wang, Y., et al., *Aggregate of nanoparticles: rheological and mechanical properties.* Nanoscale research letters, 2011. **6**(1): p. 1-6.

73. Willcott, M.R., *MestRe Nova*. 2009, ACS Publications.

74. Avaz, S., et al., *Soft segment length controls morphology of poly (ethylene oxide) based segmented poly (urethane-urea) copolymers in a binary solvent.* Computational Materials Science, 2017. **138**: p. 58-69.